Are magnetic stripes on the Cuvier Abyssal Plain (offshore NW Australia) diagnostic of oceanic crust?

Running title: Origin of the Cuvier Abyssal Plain

Matthew T. Reeve[1], Craig Magee[1,2]*, Ian D. Bastow[1], Carl McDermott[1], Christopher A.-L. Jackson[1], Rebecca E. Bell[1], Julie Prytulak[3]

[1]Basins Research Group (BRG), Department of Earth Science and Engineering, Royal School of Mines, Prince Consort Road, Imperial College London, SW7 2BP, England, UK.
[2]School of Earth and Environment, University of Leeds, Leeds, LS2 9JT, UK.
[3]Department of Earth Sciences, University of Durham, DH1 3LE, UK

*Correspondence (c.magee@leeds.ac.uk)

Abstract

Magnetic stripes have long been used to define the presence and age of oceanic crust. However, continental crust heavily intruded by magma can record magnetic reversals akin to those observed in oceanic crust. We re-evaluate the nature of the Cuvier Abyssal Plain (CAP), offshore NW Australia, which hosts magnetic stripes and has previously been defined as oceanic crust. We use magnetic, 2D seismic reflection, and geochemical data to test whether the CAP structure and composition is consistent with unambiguous oceanic crust. We show chemical data from a basalt within the CAP, previously described as displaying an enriched MORB-like signature, actually contains evidence of contamination by continental material. We also recognise seaward-dipping reflector (SDR) sequences across the CAP.

Borehole data from overlying sedimentary rocks suggests these SDRs were emplaced in a shallow-water (<200 m depths) or sub-aerial environment. Our results indicate the CAP may not be unambiguous oceanic crust. Instead, we suggest the CAP could comprise a spectrum of heavily intruded continental crust (akin to present-day Ethiopia) through to fully oceanic crust, recording the evolution from continental rifting to progressively magma-dominated, sub-aerial to shallow-water extension. Our work supports suggestions that magnetic reversals may not be truly diagnostic of oceanic crust.

Supplementary material: Enlarged and uninterpreted versions of the magnetic data and seismic reflection lines are available at.

Development of magnetic reversal anomalies (stripes) during oceanic crust formation is fundamental to modern plate tectonic theory (e.g., Vine & Matthews 1963). Where magnetic stripes occur adjacent to passive continental margins, they are commonly interpreted to mark a basin's oldest, unambiguous oceanic crust. Such stripes have also historically been used to define the continent-ocean boundary (e.g., Talwani & Eldholm 1973; Rabinowitz & LaBrecque 1979; Veevers 1986; Eagles et al. 2015): here we define unambiguous oceanic crust as comprising layers of pillow basalts, sheeted dikes, and gabbro formed during deep-marine ($\gtrsim$2 km water depths) seafloor spreading (e.g., McDermott et al. 2018). However, continental break-up can produce broad, complex zones that have structural and geochemical traits lying somewhere between unambiguous continental crust and unambiguous oceanic crust (e.g., Skogseid et al. 1992; Symonds et al. 1998; Planke et al. 2000; Skogseid et al. 2000; Direen et al. 2007; Bastow & Keir 2011). The crustal affinity of such break-up zones is accordingly difficult to distinguish (e.g., Eagles et al. 2015). Where these so-called continent-ocean transition zones (COTZs) occur, as opposed to an abrupt continent-ocean boundary, magnetic stripes within the adjacent unambiguous oceanic crust are expected to mark the outer limit of the COTZ (e.g., Pickup et al. 1996; Direen et al. 2007; Eagles et al. 2015; Paton et al. 2017; Peron-Pinvidic et al. 2019). Using magnetic stripes to recognise and accurately map the extent and age of oceanic crust has proved critical to palinspastic and plate kinematic reconstructions (e.g., Heine & Müller 2005; Eagles et al. 2015; Causer et al. 2020). Yet linear magnetic stripes akin to those hosted by unambiguous oceanic crust have recently been identified along: (i) the onshore Afar Rift, Ethiopia in heavily intruded continental crust (Bridges et al. 2012), an area expected to eventually become a COTZ assuming full seafloor spreading develops; (ii) magma-poor passive margin COTZs offshore Iberia and Newfoundland, where magnetic anomalies are recorded by magmatic intrusion into exhumed and serpentinised mantle prior to break-up (Bronner et al. 2011); (iii) part of the magma-rich passive margin COTZ offshore NW Australia (i.e. the Gascoyne margin; Direen et al. 2008); and (iv) offshore South America where the margin comprises ‘magmatic crust’ wholly comprised of new igneous material, which differs from normal oceanic crust in that it formed via sub-aerial and/or shallow-water extension, not deep-marine spreading (Collier et al. 2017; McDermott et al. 2018). These observations suggest magnetic stripes could develop within non-oceanic crust, which questions whether they can be confidently used to diagnose seafloor spreading, detect continent-ocean boundaries, and be used as hard constraints on palinspastic and plate kinematic reconstructions (Rooney et al. 2014).

Given recent studies have shown magnetic stripes may not be diagnostic of unambiguous oceanic crust formed during deep-marine seafloor spreading (e.g., Direen et al. 2008; Bridges et al. 2012; Collier et al. 2017; McDermott et al. 2018), it is worth re-evaluating the nature of previously defined oceanic crust adjacent to passive margins. Here, we test the origin of the Cuvier Abyssal Plain (CAP), offshore NW Australia through an integrated analysis of 2D seismic reflection data from the CAP, coupled with a re-examination of published chemical data (Fig. 1). The CAP hosts well-developed magnetic anomalies distributed about an inferred spreading centre along the Sonne Ridge (Fig. 1B) (e.g., Robb et al. 2005). These anomalies, coupled with observations from seismic refraction data, have previously been used to suggest that the CAP comprises unambiguous oceanic crust (Fig. 1) (e.g., Falvey & Veevers 1974; Larson et al. 1979; Robb et al. 2005; MacLeod et al. 2017). Basalts dredged from the Sonne Ridge have been interpreted to reflect an enriched MORB-like chemistry, supporting the inference that the CAP crust is oceanic (Crawford & von Rad 1994; Dadd et al. 2015). The CAP has thus previously been defined as oceanic crust in all regional and global palinspastic and palaeogeographic reconstructions involving NW Australia (e.g., Heine & Müller, 2005; Gibbons et al., 2012).

Within our seismic reflection data we recognise multiple packages of up to ~3 km thick seaward-dipping reflector (SDR) sequences, which cumulatively extend at least ~300 km oceanwards from the continental shelf. These SDR packages are likely dominated by lavas and occasionally span several well-defined, broadly linear magnetic anomalies. Lithological and biostratigraphic data from the Deep Sea Drilling Project (DSDP) Site 263 borehole indicate sedimentary strata above these SDRs were deposited in neritic environments (<200 m water depths), implying lava emplacement was sub-aerial or shallow-water. Our reinterpretation of chemical data also indicates basalts from the Sonne Ridge contain a continental signature (e.g., Robb et al. 2005; MacLeod et al. 2017). We suggest that the CAP may not be unambiguous oceanic crust and could instead comprise a spectrum of crustal types, ranging from heavily intruded continental crust to fully magmatic crust generated during sub-aerial or shallow-water extension. We consider the CAP may define a COTZ with an outer-limit >500 km oceanwards from the previously defined passive margin boundary. Our interpretation has important implications for palinspastic and plate kinematic reconstructions involving the NW Australian margin, as well as for heat flow and basin modelling studies. More generally, or study supports the arising hypothesis that magnetic stripes may not be a unique feature of oceanic crust.

Continent-Ocean Transition Zones

Where we can study active, magma-rich continental break-up onshore in Ethiopia, the processes driving development of a possible future COTZ during the latter stage of rifting (i.e. prior to rupture) involve the localisation of extension into narrow (~20 km wide) zones that progressively become dominated by dyke intrusion (e.g., Ebinger & Casey 2001; Keranen et al. 2004; Mackenzie et al. 2005; Maguire et al. 2006; Daniels et al. 2014). In these sub-aerial and so-called 'magmatic segments', ≳50% of the crust may comprise new, intruded mafic material (Daniels et al., 2014). Along volcanic or magma-rich passive margins, COTZs commonly contain seismically isotropic, fast (>7 km s^{-1}) crust, overlain by SDR sequences of mafic volcanic products (e.g. lava flows) interbedded with sedimentary rocks emplaced within sub-aerial or shallow-water environments (e.g., Eldholm et al. 1989; Larsen & Saunders 1998; Symonds et al. 1998; Menzies et al. 2002). The COTZ crust underlying these SDR-bearing domains comprises a spectrum of stretched and heavily intruded continental crust (e.g., Eldholm et al. 1989) to 'magmatic crust' (also termed 'igneous' crust), which record processes similar to those active within Ethiopian magmatic segments (e.g., Collier et al. 2017; Paton et al. 2017; McDermott et al. 2018). Magmatic crust is structurally similar to oceanic crust but instead formed during sub-aerial or shallow-water extension along a magmatic segment, rather than deep-marine spreading at a mid-ocean ridge (e.g., Collier et al. 2017; Paton et al. 2017; McDermott et al. 2018); i.e. although the formation of magmatic crust requires the prior break-up of continental crust, we note that this event may not coincide with full continental lithospheric rupture, which necessarily involves the mantle lithosphere.

Observations from rifted margins and active rifts suggest that COTZs at magma-rich passive margins are marked by a compositional and structural spectrum, bounded by unambiguous continental and oceanic crust end-members (Fig. 2). From the landward limit of COTZs, we expect the proportion of magma intruded into continental crust to increase oceanwards (Fig. 2). As dyking localises, eventually no continental crust will remain (i.e. break-up of continental crust), and the COTZ will solely comprise igneous intrusions and extrusions emplaced along magmatic segments during sub-aerial or shallow-water extension (i.e. magmatic crust; Fig. 2) (e.g., Paton et al. 2017; McDermott et al. 2018). Because of uncertainties in data resolution and interpretation mean, it is often difficult to constrain the progression from intrusion of continental crust to the onset of magmatic crust emplacement. We therefore combine these domains and refer to them both simply as a COTZ (Fig. 2). Diminishment of the buoyant support maintaining these dense, sub-aerial or shallow-water magmatic segments will promote their subsidence (e.g., Corti et al. 2015; McDermott et al. 2018). As these magmatic segments subside to water depths of $\gtrsim$2 km, plate-spreading drives the generation of unambiguous oceanic crust, comprising layers of pillow basalts, sheeted dykes, gabbro, and oceanic mantle lithosphere (e.g., McDermott et al. 2018); i.e. full continental lithospheric rupture has occurred by this point. Across COTZs and into unambiguous oceanic crust, we may therefore expect an oceanwards reduction in the continental signature of magma chemistry as they become more MORB-like (Fig. 2).

Geological Setting

Crustal Structure and Age

The North Carnarvon Basin and South Carnarvon Basin form part of the NW Australian magma-rich passive margin, bound by the Argo Abyssal Plain to the north, and the Gascoyne Abyssal Plain and Cuvier Abyssal Plain (CAP) to the west (Fig. 1A) (Longley et al. 2002;

Stagg et al. 2004). Basin formation occurred during multiple phases of Permian-to-Late Jurassic rifting, culminating in Early Cretaceous break-up of the Gascoyne and Cuvier margin rift segments (Fig. 3A) (Longley et al. 2002). We sub-divide the study area into the ~400 km wide Gascoyne and 180 km-wide Cuvier margin sectors, separated by the NW-trending Cape Range Fracture Zone (Fig. 1A). The CAP is bound to the SW by the Wallaby Plateau and Wallaby Saddle (Fig. 1A).

Previously interpreted continent-ocean transition zones (COTZs)

A 200–250 km wide COTZ lies northwest of the continental Exmouth Plateau (i.e. the Gallah Province; Fig. 1A). This COTZ comprises 2–5.5 km thick SDRs and high-velocity lower crust (Direen et al. 2008). The Gallah Province COTZ preserves magnetic stripes formed during chrons M10N–M5n (~136–131 Ma; Valanginian-to-Hauterivian), with interpreted oceanic crust (Gascoyne Abyssal Plain) emplaced onwards from chron M3r (~130 Ma, Hauterivian; Figs 1B and 3A) (Direen et al. 2008). Along the Cuvier Margin, beneath the modern continental slope, seismically imaged SDR sequences are interpreted to mark a 50–70 km wide COTZ (e.g., Figs 1A and C) (Hopper et al. 1992; Symonds et al. 1998).

Cuvier Abyssal Plain

Adjacent to the Cuvier Margin, the CAP lies ~5 km below sea level and comprises a ~1–3.3 km thick sedimentary sequence overlying ~6–10.5 km thick crystalline crust (e.g., Fig. 1C) (Hopper et al., 1992). Based on recognition of magnetic chrons M10N–M5 within the CAP, it has been interpreted as oceanic crust emplaced initially at ~136 Ma (i.e. Valanginian; Figs 1B and 3A) (Falvey & Veevers 1974; Larson et al. 1979). The presence of chrons M10N–M5 within the Gallah Province COTZ (Direen et al. 2008) and the inference that seafloor spreading began in the CAP at ~136 Ma, suggest that continental rupture and seafloor spreading adjacent to the Cuvier Margin occurred ~5–6 Myr before the Gascoyne Margin (Fig. 3A) (Falvey & Veevers 1974; Larson et al. 1979). Critically, the occurrence of magnetic stripes in the non-oceanic (i.e. COTZ) crust of the Gallah Province questions whether the presence magnetic stripes in the CAP should be used to classify it as oceanic crust (e.g., Direen et al. 2008; Bridges et al. 2012; Collier et al. 2017; McDermott et al. 2018).

Origin of the Sonne and Sonja ridges

Under the assumption that the CAP comprises oceanic crust, the ~175 km long Sonne Ridge and ~100 km long Sonja Ridge, which extend into the Wallaby Plateau (Fig. 1A), have been interpreted as probable extinct oceanic spreading ridges (e.g., Mihut & Müller 1998; Robb et al. 2005; MacLeod et al. 2017); in this model, spreading is interpreted to have jumped from the Sonne Ridge to the Sonja Ridge at ~131.7 Ma (Hauterivian). Geochemical analyses of a basalt dredged from the Sonne Ridge along its extension into the Wallaby Plateau, suggest it has a slightly enriched MORB-like signature, supporting the inference that the Sonne Ridge is an oceanic spreading centre (Dadd et al. 2015). An alternative interpretation forwarded for the Sonne Ridge is that it represents a ‘pseudofault’ (i.e. an apparent offset in magnetic stripes formed by ridge jumps; Hey 1977); this interpretation is based on changes in gravity intensity across the structure and the possible termination of the Cape Range Fracture Zone directly north of the ridge (Gibbons et al. 2012). In their model, Gibbons et al. (2012) define a different oceanic spreading centre ~100 km to the SE and parallel to the Sonne Ridge (red dashed line in Figs 1A and B). However, we note that Gibbons et al. (2012) use the COB of Heine & Müller (2005) to define the termination of the Cape Range Fracture Zone. This COB interpretation does not consider the Gallah Province is a COTZ and, hence, does not include the required north-westward extension of the fracture zone beyond the seaward limit of the Exmouth Plateau (Heine & Müller 2005; Robb et al. 2005; Direen et al. 2008). Overall, given the repetition of magnetic stripe sequences either side of the Sonne Ridge, and to a lesser extent the Sonja Ridge, we favour their interpretation as spreading ridges and thus use the interpreted magnetic chron configuration of Robb et al. (2005). This magnetic chron configuration is centred on the Sonne Ridge and predicts half-spreading rates adjacent to both Gascoyne and Cuvier margins were similar during chrons M10–M5 (~4.5 cm/yr), decreasing to ~3 cm/yr by chron M3 (Robb et al. 2005).

The Wallaby Plateau and Wallaby Saddle

The Wallaby Plateau is a large bathymetric high (Fig. 1A), containing up to ~7.5 km thick sequences of volcanic and sedimentary rocks, which are typically expressed in seismic reflection data as packages of diverging and dipping reflections that appear similar to SDRs (e.g., Colwell et al. 1994; Daniell et al. 2009; Stilwell et al. 2012; Olierook et al. 2015). Interpretation of seismic reflection and magnetic data, coupled with chemical, geochronological, and biostratigraphic analyses of dredge samples, suggests the Wallaby Plateau probably comprises ~124 Myr old, continental flood basalts and interbedded sedimentary strata emplaced on a fragment of extended continental crust (see Olierook et al. 2015 and references therein). Between the Wallaby Plateau and the Australian continent is the Wallaby Saddle, a bathymetric low containing SDRs but no magnetic stripes, interpreted by Symonds et al. (1998) to comprise ‘transitional’ crust (Figs 1A and B). The Wallaby Plateau and Wallaby Saddle seemingly preserve a range of crustal types typical of a COTZ, but not unambiguous continental crust or unambiguous oceanic crust. Similarities between their structure and that of the CAP may therefore imply the latter is not truly oceanic crust.

Sedimentary Cover on the Cuvier Abyssal Plain

The top of the crystalline basement within the CAP corresponds to a high-amplitude reflection in seismic data, which is overlain by a ~1–3.3 km thick, sedimentary succession broadly comprising sub-horizontal reflections (e.g., Fig. 1C) (e.g., Veevers & Johnstone 1974; Hopper et al. 1992). Biostratigraphic and lithological data for the sedimentary cover are available from the DSDP Site 263 borehole, which was drilled in 1972 and terminates ~100–200 m above the basement (Figs 1A and 3B) (e.g., Bolli 1974; Scheibnerová 1974; Wiseman & Williams 1974; Holbourn & Kaminski 1995). From a depth of 200 m below seabed to the base of the borehole (746 m), the sedimentary strata intersected at DSDP Site 263 comprise black claystones; between depths of ~475–746 m these claystones are silty and contain abundant kaolinite (Fig. 3B) (Robinson et al. 1974; Compton et al. 1992). Within the lowermost ~20 m of the drilled sequence, and in thin units at around ~500 m depth, the siltstones occur that are poorly sorted, and contain angular quartz grains (Fig. 3B) (Robinson et al. 1974). Analyses of benthic foraminifera from DSDP Site 263 suggest the black, kaolinitic claystones spanning ~475–746 m are likely Hauterivian-to-Middle Barremian, passing upwards into Albian-to-Aptian black claystones (Fig. 3B) (Holbourn & Kaminski 1995); these age ranges are supported by dinoflagellate distributions and carbon isotope stratigraphy (Wiseman & Williams 1974; Oosting et al. 2006). A gradual upwards transition from coarsely to finely agglutinated foraminifera species, coupled with an upwards increase in the scarcity of shallow-water taxa (e.g., *Hyperamina* spp.) and a corresponding decrease in grain size, suggests that the Hauterivian-to-Middle Barremian strata record deepening neritic (i.e. <200 m water depth) conditions (e.g., Fig. 3B) (Robinson et al. 1974; Veevers & Johnstone 1974; Holbourn & Kaminski 1995; Oosting et al. 2006). Sedimentary rocks recovered from the Pendock-1 borehole, which is located on the current continental shelf, are sedimentologically similar and of comparable age to those penetrated in DSDP 263 (Veevers & Johnstone 1974; Holbourn & Kaminski 1995). These similarities to Pendock-1 suggest that the Hauterivian-to-Middle Barremian strata sampled by DSDP Site 263 can broadly be correlated to the Winning Group of the North and South Carnarvon basins (Figs 1A and 3) (Veevers & Johnstone 1974; Holbourn & Kaminski 1995).

Dataset and methodology

Seismic reflection data

To assess the crustal structure of the CAP and surrounding areas, we interpret seven 2D seismic lines from four, pre-stack time-migrated reflection surveys (Fig. 1A) (see Supplementary Table 1 for acquisition and processing details for each survey). Seismic lines EW0113-5, EW0113-6, and repro-n303 are each >400 km long and extend from the continental shelf up to ~300 km into the CAP from the currently defined COTZ (i.e. they are orthogonal to the structural trend of the margin); EW0113-5 and EW0113-6 span the mapped area of SDRs in the Cuvier COTZ and the location of the extinct spreading centre predicted by Gibbons et al., (2012), whereas repro-n303 images the Sonne Ridge (Fig. 1A). Due to extreme amplitude contrasts between the shallow and deep sections of the original migrated, EW0113 data, we applied a time-dependent gain filter and root filter to improve amplitude balance and enhance deep reflectivity (see supplementary information for details). Lines s135-05, s135-08, and s310-59 image the inferred ‘transitional’ crust of the Wallaby Saddle and the intruded continental crust of the Wallaby Plateau (e.g., Symonds et al., 1998; Goncharov and Nelson, 2012; Olierook et al., 2015). The NE-trending seismic line s135-11 was also interpreted as ties together the margin-orthogonal seismic lines and provides a margin-parallel image of the southernmost Exmouth Plateau continental crust, the CAP, and the Wallaby Plateau (Fig. 1A).

Although time-migrated seismic reflection data allows us to qualitatively and quantitatively characterise crustal structure, seismic velocity information is required to convert depth information from seconds two-way time (TWT) to metres. To provide context for the thicknesses and depths of some discussed structures, we depth-converted the EW0113-5 and EW0113-6 seismic data using interval velocities derived from ocean-bottom seismometer (OBS) data (Table 1) (Tischer 2006). The OBS array was co-located with seismic line EW0113-6, which is located ~70 km along-strike from line EW0113-5 (Fig. 1A); the geological structure imaged in line EW0113-6 is very similar to that of EW0113-5, supporting the use of velocities from EW0113-6 to depth convert both lines. As velocity data from across the Wallaby Plateau and Wallaby Saddle is limited (Goncharov & Nelson 2012), and because along-strike variation in geology will likely promote changes in the velocity structure, lines s135-05, s135-08, and s310-59 are presented in time. For easier comparison between seismic data from the CAP and the Wallaby Plateau and Wallaby Saddle, we do not depth-convert repro-n303 or s135-11. Interpretation of reflection configurations (e.g., dip values) in time-migrated data are only qualitative, and may change if depth-converted.

Magnetic data

To examine the regional magnetic anomalies, we utilise the EMAG2v2 and EMAG2v3 Earth Magnetic Anomaly Grids (Maus et al. 2009; Meyer et al. 2017). EMAG2v2 is a 2 arc min resolution grid derived from marine, airborne, and satellite magnetic data, but uses *a priori* information to interpolate magnetic anomalies in areas where data gaps are present (Fig. 4A) (Maus et al. 2009; Meyer et al. 2017). In contrast, EMAG2v3 uses more data points to derive magnetic anomaly maps but assumes no *a priori* information (Fig. 4B) (Meyer et al. 2017). In ocean basins with a relatively poor coverage of magnetic data available, such as the CAP, clear linear magnetic anomalies in EMAG2v2 thus typically appear poorly developed or are absent in EMAG2v3 (cf. Figs 4A and B) (Meyer et al. 2017). This difference in the presence and appearance of linear magnetic anomalies between grids is because (assumed) knowledge of seafloor spreading processes was incorporated into, and therefore influenced, interpolation during construction of the EMAG2v2 grid (Maus et al. 2009; Meyer et al. 2017). Importantly, the apparent reduction in magnetic stripes observed in EMAG2v3, compared to EMAG2v2 (Figs 4A and B), does not necessarily mean these features are absent, but rather that the available data is insufficient to unambiguously confirm their presence in non-directionally gridded data such as EMAG2v3 (Meyer et al. 2017). Comparing the EMAG2v2 and EMAG2v3 grids, coupled with shiptrack magnetic data (Robb et al. 2005), allows us to interrogate the magnetic architecture of the CAP (cf. Meyer et al. 2017). In particular, we use EMAG2v2 to interpret possible magnetic chrons, picked on positive peaks (Fig. 1B), and attempt to correlate them to the EMAG2v3 grid and shiptrack magnetic data. From these comparisons, we tied interpreted magnetic stripes to seismic line EW0113-5, EW0113-6, and repro-n303 using the synthetic profiles of Robb et al. (2005). To update the absolute ages of the interpreted magnetic anomalies (Robb et al. 2005), we use the time-calibrated, magnetic polarity reversal sequence of Gradstein & Ogg (2012).

Geochemical data

To evaluate whether the Sonne Ridge is an extinct seafloor spreading centre (e.g., Mihut & Müller 1998; Robb et al. 2005) consisting of oceanic crust with a MORB or MORB-like affinity along its length, we examine chemical data from a dredged basalt lava sample collected along its extension into the Wallaby Plateau (i.e. Site 57 - sample 057DR051A; diamond 57 in Fig. 1A) (Daniell et al. 2009; Dadd et al. 2015; Olierook et al. 2015). We compare the Sonne Ridge sample to two samples collected from near the south-western margin of the Wallaby Plateau (diamonds 55 and 52 in Fig. 1A) (i.e. Site 55 - samples 055BS004A and 055BS004B) (Dadd et al. 2015). Two Wallaby Plateau basalts dated from Site 52 (Fig 1A) yield plagioclase $^{40}Ar/^{39}Ar$ plateau ages of 125.12±0.9 Ma and 123.80±1.0

Ma, whereas two analyses of the Sonne Ridge sample yielded less precise ages of 120±14 Ma and 123±11 Ma (Olierook et al. 2015).

Results

Reflection seismology

Cuvier Abyssal Plain

We interpret a prominent, continuous, high-amplitude seismic reflection across the CAP; this represents the interface between crystalline rock and overlying sedimentary strata (e.g., Figs 1C and 5). The Moho was picked at the base of a sub-horizontal zone of moderate-to-high-amplitude, discontinuous seismic reflections, and is broadly flat-lying at ~16–17 km or ~10 s TWT (Fig. 5). On EW0113-5, the Moho appears to become shallower oceanwards (to ≤14 km), although our interpretation of repro-n303 suggests it may deepen again beneath the Sonne Ridge (Figs 5A and D). Overall, the crystalline crust is ~8–10 km (~3–5 s TWT) thick (Figs 1C and 5). On EW0113-5 and EW0113-6, there is no clear evidence for the spreading ridge interpreted by Gibbons et al., (2012), which is expected to occur within magnetic chron M9n (Figs 1A and 5).

Across the CAP, the ~1–3 km-thick, uppermost crystalline crustal layer comprises a layered, moderate- to high-amplitude seismic facies (SF1; Fig. 5). On NW-trending seismic lines orthogonal to the margin (i.e. EW0113-5, EW0113-6, and repro-n303), SF1 locally contains ≤40 km wide, ≤4.5 km thick wedges of coherent, high-amplitude, dipping reflections that predominantly diverge seaward (Figs 5 and 6); adjacent to the Sonne Ridge on its NW side, a package of dipping reflections diverge landwards (e.g., Fig. 5D). There is no correlation between the location and width of these wedges relative to the magnetic chrons; e.g., some packages of seaward-diverging reflections span several chrons (Fig. 5). Where well-developed wedges are absent, SF1 contains discontinuous, horizontal to gently seaward-dipping reflections (Fig. 5). On line s135-11, which is oriented parallel to the margin, most reflections within SF1 are either sub-horizontal or dip gently north-eastwards (Fig. 7). Seismic velocities for SF1 are estimated to be ~4–5 km/s (Fig. 5; Tischer 2006).

In places, the uppermost crystalline layer (SF1) is underlain by a low-amplitude, near transparent seismic facies (i.e. SF2), which is particularly clear on lines EW0113-5 and EW0113-6 (Figs 5 and 6). SF2 is up to ~2.8 km thick, being thinnest and occasionally absent beneath wedges of dipping reflections within SF1 (Figs 5 and 6). The few reflections that occur within SF2 typically have low-to-moderate to amplitudes and variable dips (Figs 5 and 6). On repro-n303, at the seaward termination of an overlying wedge in SF1, a ~15 km wide swarm of landward-dipping reflections are present in SF2 (Fig. 5D). There is no clear SF2 observed on line s135-11, even in areas where it is encountered on the intersecting margin-orthogonal lines (Fig. 7).

Beneath SF2 we recognise a ~3.5–6 km (<2 s TWT) thick, low-amplitude layer that locally contains prominent, high-amplitude, dipping reflections and discontinuous, moderate amplitude, sub-horizontal reflections (SF3; Figs 5–7). On line EW0113-5, the inclined reflections within SF3 terminate at the Moho and primarily dip oceanwards at 20–30° (Fig. 5A). On lines EW0113-6 and repro-n303, however, reflections within SF3 dip both oceanwards and landwards (Figs 5B, C, and 6). Mapped reflections within SF3 on s135-11 primarily dip towards the SE, extending from the top of the layer down into the mantle, cross-cutting but not offseting NE-dipping, gently inclined reflections (Fig. 7). Similar mid- and lower-crustal reflection configurations to SF2 and SF3, respectively, occur in the seismic data presented by Hopper et al. (1992) (Fig. 1C). Seismic velocities of SF2 and SF3 are 6.8–7.2 km/s (Fig. 4; Tischer 2006).

Wallaby Plateau and Wallaby Saddle

Building on previous investigations of seismic data across the continental-to-COTZ crust of the Wallaby Plateau and Wallaby Saddle, here we (re)interpret several 2D seismic lines and compare their structure to that of the CAP. Similar to the CAP, a prominent, continuous, high-amplitude seismic reflection marks the interface between crystalline rock and overlying sedimentary strata across the Wallaby Plateau and Wallaby Saddle (Figs 7 and 8). Within the Wallaby Saddle, the crust appears to be ~5–6 s TWT thick, although the Moho can only tentatively be interpreted, and can also be sub-divided into: (i) SF1, itself containing up to ~4 s TWT thick, 12 km wide wedges of diverging reflections that typically dip seawards; (ii) restricted zones that seismically appear similar to SF2 described from the CAP; and (iii) a 1.5–3 s TWT thick SF3 unit that contains reflections with variable dips, including prominent swarms of landward-dipping reflections that cross-cut but do not offset other reflections and that typically occur at the oceanward termination of SF1 wedges (Fig. 8). Derivation of interval velocities from seismic reflection stacking velocities suggests rocks comprising SF1 have velocities of ~2.5–5.3 km s^{-1} (see insets in Fig. 8C) (Goncharov & Nelson 2012). It is difficult to determine whether SF1-SF3 continue across the full extent of the Wallaby Saddle in s310-59 because there appears to be a distinct change in reflection configuration (Fig. 8C). In particular, we observe that although reflectivity in west of this change is decreased, reflections towards the top of the crust are broadly sub-parallel to the basement reflection and those within the mid- to lower-crustal areas are either gently inclined landwards, or moderately inclined oceanwards (Fig. 8C).

Seismic reflection imaging of the Wallaby Plateau reveals the crust is up to ~7 s TWT thick (e.g., at the Sonne Ridge), thicker than that of the Wallaby Saddle (~5–6 s TWT thick) but that there is no apparent significant change in Moho depth between the two crustal domains (Figs 7 and 8); we note these observations are based on time-migrated data and may thus be invalidated if there any differences in velocity structure between the two areas not previously recognised. The crust of the Wallaby Plateau is also thicker than that of the CAP, and its underlying Moho is located at deeper levels (~12 s TWT; Fig. 7). Towards the SW margin of the Wallaby Plateau, a ~40 km wide, apparently NE-trending rift system occurs, comprising normal faults with throws of up to ~1 s TWT that bound and dissect a graben (Figs 8B–D). Reflections within the upper section of the Wallaby Plateau crust are typically moderate-to-high amplitude and form layered packages, which are either conformable to the top basement horizon or that diverge (Fig. 8). The diverging packages of dipping reflections appear similar to SF1 observed in the CAP and Wallaby Saddle (Figs 5 and 8). Derivation of interval velocities from seismic reflection stacking velocities suggests rocks comprising these diverging reflector sequences have velocities of ~2.5–5.3 km s^{-1} (Fig. 8C) (Goncharov & Nelson 2012). Due to uncertainties regarding the reliability of seismic processing within the middle and lower crustal sections of the Wallaby Plateau, e.g., where imaging is hindered by seabed multiples, it is difficult to confidently interpret reflections as real geological features and not artefacts. However, we note that in these middle and lower crustal sections, reflections are low-to-moderate amplitude and broadly dip gently in various directions; in places, steeply inclined reflections are observed that appear to cross-cut but not offset gently dipping reflections (Fig. 8). These steeply inclined mid- to lower-crustal reflections typically appear to be located beneath diverging reflection packages, or beyond their down-dip termination (Fig. 8).

Comparison of magnetic anomalies to seismic reflection data

EMAG2v2 and ship-track magnetic data reveal that 10 km wide, ≤220 km long magnetic stripes cover much of the CAP (Figs 1B, 4, and 5). No magnetic stripes can confidently be identified and dated within the Wallaby Plateau and none are observed within the Wallaby Saddle (Figs 1B and 4). Although magnetic anomalies in the EMAG2v3 grid are suppressed relative to EMAG2v2, subtle, linear anomalies can still be distinguished across the CAP and in the Gallah Province (cf. Figs 4A and B). Due to the lower resolution of magnetic anomalies in the EMAG2v3 grid, magnetic chrons cannot be confidently attributed and we thus rely on EMAG2v2 and shiptrack data to define possible chrons (Fig. 4). Proximal to the Australian continent, long-wavelength magnetic anomalies can only be broadly assigned to chron M10N (~135.9–134.2 Ma; Figs 1B, 4, and 5) (Robb et al. 2005); across parts of seismic lines EW0113-5, EW0113-6, and repro-n303, chrons M10n–M5r (~135.3–131.4 Ma) are clearly defined and have amplitudes of ≤±100 nT (Figs 1B, 4, and 5). On all three seismic lines, chrons M8r–M7n (~133–132 Ma) coincide with a package of seaward-dipping reflectors observed in SF1, which on EW0113-5 is ≤3 km thick and ~25 km long (Fig. 5).

Robb et al. (2005) interpret the magnetic anomalies M10N–M6 southeast of the Sonne Ridge as conjugate to a more poorly developed set of anomalies northwest of the ridge (Fig. 1B). These chrons NW of the Sonne Ridge (i.e. M10N–M6; ~135.9–131.7 Ma) terminate abruptly north-eastwards against the Cape Range Fracture Zone, abutting magnetic chrons on the Gallah Province, and to the SW are cross-cut by chrons (M5n?; 131.7–130.6 Ma) mirrored either side of the Sonja Ridge (Fig. 1B). Beyond the outermost chron (M10N) interpreted in the CAP, chron M5n is the first to occur continuously along-strike across both the Cuvier and Gascoyne margin segments, extending into the Wallaby Plateau (Fig. 1B).

Geochemistry of basalts dredged from the Sonne Ridge

The only basalt collected from the Sonne Ridge displays a relatively flat Rare Earth Element (REE) pattern (Fig. 9A). Based on this observation, Dadd et al. (2015) interpret the basalt to have a slightly enriched MORB-like source, supporting the inference that the CAP comprises oceanic crust (e.g., Larson et al. 1979; Hopper et al. 1992; Mihut & Müller 1998). Although a flat REE pattern can be indicative of a shallow melting regime related to MORB generation, it does not preclude other settings. By replotting the trace element and radiogenic isotopic compositions of the Sonne Ridge sample, we show the sample has characteristics that could suggest a more continental source (Fig. 9A). It should be noted that the Sonne Ridge sample is heavily altered (Dadd et al. 2015) which could explain the elemental enrichment in Pb, Ba, and Rb, as well as elevated $^{87}Sr/^{86}Sr$. However, the sample exhibits unradiogenic ε_{Nd} and a negative Nb anomaly that is in part defined by a relative enrichment in the neighbouring element Th, which likely cannot be attributed to contamination; the combination of these features likely cannot be ascribed to alteration (Fig. 9). Instead, the negative Nb anomaly and unradiogenic ε_{Nd} may indicate a chemically evolved, continental or sedimentary contribution to the magmas. The chemical similarity of the Sonne Ridge basalt to two ~124 Ma samples from the Wallaby Plateau (Fig. 9), which is interpreted to comprise intruded continental crust (Daniell et al. 2009; Stilwell et al. 2012; Olierook et al. 2015), is also consistent with a continental or sedimentary contribution to the Sonne Ridge magmas.

Interpretation and Discussion

Since the recognition that it contains magnetic stripes, the CAP has been considered to comprise unambiguous oceanic crust that formed at ~136 Ma (Valanginian) in response to seafloor spreading at the Sonne Ridge (e.g., Falvey & Veevers 1974; Larson et al. 1979; Hopper et al. 1992; Robb et al. 2005). An oceanic origin for the CAP has been supported by seismic reflection-based observations that it has a thin crust relative to adjacent continental blocks (e.g., Fig. 1C) (e.g., Hopper et al. 1992), and chemical data, which suggest it has a MORB-like signature (Dadd et al. 2015). The apparent certainty that the CAP is oceanic means it has been unquestionably treated as such in all geological models of the evolution of NW Australia, including regional and global palinspastic and plate kinematic reconstructions (Heine & Müller 2005; Gibbons et al. 2012). However, the identification of linear magnetic anomalies within non-oceanic crust, in areas such as Ethiopia and the Atlantic margins, requires us to re-evaluate the origin of crustal domains previously classified as oceanic crust based on the presence of magnetic stripes (e.g., Bronner et al. 2011; Bridges et al. 2012; Collier et al. 2017; McDermott et al. 2018).

Seismic facies interpretation

Beneath the sedimentary cover across the CAP, we recognise three distinct layers (SF1–SF3; Figs 5–8). We particularly identify a newly recognised upper-crustal layer (SF1) in the CAP that comprises well-developed wedges of divergent, seaward-dipping reflectors (SDRs) (Figs 5 and 6). These SDRs are ≤4.5 km thick, likely have seismic velocities of ~4–5 km s^{-1} (Tischer 2006), and that collectively extend >300 km seaward from the previously interpreted COTZ (Figs 5 and 6). Diverging SDRs are also observed within the: (i) the previously defined, 50–70 km wide COTZ along the Cuvier Margin beneath the continental slope, where they are up to ~5 km thick (e.g., Fig. 1C) (e.g., Hopper et al. 1992; Symonds et al. 1998); and (ii) across the Wallaby Saddle and Wallaby Plateau, where they are ~5–10 km thick and have similar seismic velocities (2.5–5.3 km s^{-1}) to those in the CAP (Figs 5, 6, and 8) (e.g., Symonds et al. 1998; Sayers et al. 2002; Goncharov & Nelson 2012). The lack of boreholes penetrating these SDR sequences offshore NW Australia means we cannot determine their composition or the nature of underlying crust. However, SDR sequences that are geometrically and geophysically (e.g., seismic velocities typically range from ~3–5 km s^{-1}) similar to those from offshore NW Australia (e.g., SF1) have been recognised along other passive margins, developed on both heavily intruded continental crust and thickened oceanic crust (e.g., Hinz 1981; Larsen & Saunders 1998; Harkin et al. 2020). Where these SDRs have been drilled, or are exposed onshore (e.g., Iceland and Greenland), they comprise interbedded basaltic lavas, tuffs, and sedimentary rocks formed during sub-aerial, or perhaps shallow-water, continental breakup and crustal spreading (e.g., Bodvarsson & Walker 1964; Mutter et al. 1982; Roberts et al. 1984; Eldholm et al. 1987; Larsen et al. 1994a; Geoffroy et al. 2001; Harkin et al. 2020). Based on similarities in structure and seismic velocities to SDRs studied elsewhere, we suggest that SF1 comprises spreading-related volcanic rocks interbedded with sedimentary layers (Figs 1C, 5, 6, and 8) (e.g., Mutter et al. 1982; Hopper et al. 1992; Symonds et al. 1998; Planke et al. 2000; McDermott et al. 2019; Harkin et al. 2020).

SDR sequences (SF1) can develop on heavily intruded continental crust or thickened oceanic crust (e.g., Larsen & Saunders 1998). The observed structure and seismic velocities (6.8–7.2 km s^{-1}) of SF2 and SF3 in the CAP, defined by transparent seismic facies and discordant high-amplitude reflections, respectively (Figs 5–8), are consistent with the typical seismic character of sheeted dykes and lower crustal gabbro intrusions in oceanic crust (e.g., Eittreim et al. 1994; Paton et al. 2017). However, we note that these seismic facies are not uniquely diagnostic of oceanic crust but can also occur in COTZs, where moderate- to high-amplitude reflections may represent igneous intrusions (e.g., dykes), primary layering within gabbros, or texturally distinct lower crustal shear zones within otherwise homogenous crystalline rocks (e.g., Phipps-Morgan & Chen 1993; Abdelmalak et al. 2015; Paton et al. 2017). For example, the swarm of landward dipping reflections within SF2 and SF3 at the down-dip termination of an SDR sequence may correspond to dykes; i.e. they cross-cut but do not offset background reflections and are thus not faults or shear zones (e.g., Figs 5 and 8) (e.g., Abdelmalak et al., 2015; Phillips et al., 2018).

Implications of SDR recognition for the CAP

Origin of SDR lavas

Lavas within SDR wedges are inferred to emanate from and be thickest at axial magmatic segments, where they were likely fed by sub-vertical dykes. With continued plate divergence, these lavas subside and rotate to dip inwards towards their eruption site (e.g., Planke & Eldholm 1994; Paton et al. 2017; Norcliffe et al. 2018; Tian & Buck 2019); this subsidence also rotates underlying feeder dykes, which will dip away from the magmatic segment (e.g., Lenoir et al. 2003; Abdelmalak et al. 2015). SDRs across the CAP appear to dip and diverge north-westwards, except one SDR-like package of concave-upwards reflections that borders and diverges south-eastwards towards the Sonne Ridge; i.e. we define a conjugate set of SDRs that occur either side of and dip towards the Sonne Ridge (Fig. 5). Although only one SDR package to the NW of the Sonne Ridge dips south-eastwards towards the ridge, we suggest that the other SDR packages, which dip north-westwards, relate to and were formed at the Sonja Ridge (Fig. 5). From these SDR geometries and distribution, coupled with the previously inferred conjugate sets of magnetic chrons (Fig. 1B), our results are consistent with suggestions that (Falvey & Veevers 1974; Larson et al. 1979; Robb et al. 2005; MacLeod et al. 2017): (i) extension within the CAP was predominantly centred on the Sonne Ridge during chrons M10N–M5r (~136–131 Ma); before (ii) briefly jumping to the Sonja Ridge at ~131 Ma (chron M5n), which interrupted subsidence and rotation of the SDR wedge immediately to the NW of the Sonne Ridge and instead produced north-westwards diverging SDRs. There are no changes in SDR divergence direction either side of chron M9n in EW0113-5 or EW0113-6, suggesting no spreading centre existed here (Figs 5A and B) (cf. Gibbons et al. 2012).

The chemistry of a basalt sample from the Sonne Ridge, particularly its Nd isotopic composition and refractory trace element abundances (Fig. 9), indicates it could originate from either: (i) melting of sub-continental lithospheric mantle (SCLM); or (ii) contamination of a MORB-like magma by assimilation as it ascended through continental crust (cf. Dadd et al. 2015). Because these chemical data provide evidence that the Sonne Ridge basalt interacted with continental material, these same data cannot thus be used as definitive evidence that the CAP comprises oceanic crust (cf. Dadd et al. 2015). The basalt sample dredged from its present-day bathymetric expression can be considered a product of one of the youngest magmas within the CAP system (e.g., Robb et al. 2005). We thus think it plausible that older magmas emanating from the Sonne Ridge, including the SDRs imaged in the seismic reflection data, could have a more pronounced continental signature.

Environment of SF1 lava emplacement

Borehole and field data reveal SDR lavas typically erupt sub-aerially, but can develop sub-aqueously (e.g., Bodvarsson & Walker 1964; Mutter et al. 1982; Roberts et al. 1984; Eldholm et al. 1987; Larsen et al. 1994b; Symonds et al. 1998; Planke et al. 2000; Geoffroy et al. 2001; Harkin et al. 2020). Determining the environment and age of SDR deposition can help establish whether they likely formed via: (i) seafloor spreading at a mid-ocean ridge, consistent with previous interpretations that the CAP comprises unambiguous oceanic crust (e.g., Falvey & Veevers 1974; Larson et al. 1979; Hopper et al. 1992; Robb et al. 2005); or (ii) magmatic addition along a sub-aerial or shallow-water axis during the transition from continental rifting to full plate separation (i.e. the CAP does not comprise oceanic crust) (e.g., McDermott et al. 2018). However, from their seismic character alone it can be difficult to determine whether SDRs formed in sub-aerial, shallow-water, or deep-marine environments (e.g., compare inner and outer SDR character and inferred emplacement conditions; Symonds et al. 1998; Planke et al. 2000).

Observations from the DSDP Site 263 borehole, which terminates ~100–200 m above the crystalline crust, indicate the sedimentary cover deposited above the SDRs: (i) comprises poorly sorted silty claystones that include angular quartz grains and abundant kaolinite, consistent with a neritic (i.e. <200 m water depth) depositional environment (Fig. 3B) (e.g., Robinson et al. 1974; Veevers & Johnstone 1974; Compton et al. 1992; Holbourn &

Kaminski 1995; Oosting et al. 2006); (ii) contain coarsely agglutinated foraminifera species and taxa such as *Hyperamina* spp. within the lowermost intersected strata, which are typical of shallow-marine conditions (Holbourn & Kaminski 1995); and (iii) based on biostratigraphic data were deposited at least in the middle Barremian (e.g., ~127 Ma), but are perhaps as old as Hauterivian (~132.6–129.4 Ma) (Oosting et al. 2006). Deposition of the lowermost sedimentary cover intersected by DSDP Site 263 thus occurred up to ~9 Myr (i.e. ~135.9–127 Ma) after formation of the CAP crust they rest upon, which records chron M10N (135.9–134.2 Ma), during development of crust hosting chrons M7–M1n (132.5–126.3 Ma; Fig. 1B). Critically, SDR-bearing crust cools and subsides as it is transported away from its emplacement site (e.g., Planke & Eldholm 1994; Paton et al. 2017; Norcliffe et al. 2018; Tian & Buck 2019). The presence of strata deposited in the neritic zone (<200 m water depth) above SF1 in DSDP 263, after ~9 Myr of crustal cooling and subsidence, thus implies lava eruption during the early stages of CAP formation occurred: (i) in a sub-aerial or shallow-water environment (i.e. comparable to the inner SDRs of Symonds et al. 1998; Planke et al. 2000), if we assume the underlying crust only subsided in the ~9 Myr between SDR emplacement and sediment deposition; or (ii) at a moderately deep-marine spreading centre (i.e. comparable to the outer SDRs of Symonds et al. 1998; Planke et al. 2000), but localised uplift elevated the DSDP 263 area to bathymetric depths equivalent to the neritic zone prior to deposition of overlying strata. We lack the data from strata directly overlying or interbedded with the SDRs to test these two interpretations regarding lava emplacement depth, but note that the relatively flat-lying crystalline crust across the interpreted CAP seismic lines (except for the Sonne Ridge) provides no evidence of post-spreading uplift, perhaps suggesting a sub-aerial or shallow-water environment of emplacement is most plausible (Fig. 5).

Nature of CAP crust

Seismic and magnetic data alone are insufficient to determine the origin of the CAP crust because the SDRs, seismic facies (SF1–SF3), and magnetic stripes these data illuminate can be recognised in both oceanic crust and COTZs (e.g., Larsen & Saunders 1998; Symonds et al. 1998; Planke et al. 2000; Bridges et al. 2012; Collier et al. 2017; McDermott et al. 2018). We also show that the chemical data available for a basalt at the Sonne Ridge possesses a continental signature and are thus inconclusive regarding whether or not the crust is oceanic (Fig. 9) (cf. Dadd et al. 2015). However, based on lithological and biostratigraphic data from the sedimentary cover intersected by DSDP Site 263, we suggest: (i) the inferred lavas within SF1, at least during the early stages of CAP formation (i.e. chron M10N), likely erupted in a sub-aerial, or perhaps shallow-water (<200 m water depth), environment; and (ii), assuming the underlying crystalline crust had since subsided relative its position during formation, that the syn-depositional, ~9 Myr old Sonne Ridge was elevated above at least the base of the neritic zone. These constraints on SDR emplacement depth are inconsistent with the CAP being oceanic crust since mid-ocean ridges in such a setting are expected to occur at water depths of ~3 km after 5–10 Myr of spreading (e.g., Menard 1969; Parsons & Sclater 1977; Stein & Stein 1992).

We envisage that crustal structure of the CAP could involve a gradual north-westwards change from the continental crust of the Cuvier Margin into a COTZ, which is likely characterised at its landward edge by heavily intruded continental crust and progressively becomes increasingly magma-dominated towards the Sonne Ridge (Figs 2 and 10). Our data are insufficient to determine where, or if, there is a transition from heavily intruded continental crust to magmatic crust, which would mark break-up of the continental crust within the CAP. Repetition of the M10N-M6 chrons centred on the Sonne Ridge suggests the possible COTZ of the CAP may extend at least out to chron M5n, which is: (i)

>500 km oceanwards of the outer- limit of the previously defined Cuvier COTZ (e.g., Hopper et al. 1992; Symonds et al. 1998); and (ii) broadly coincident with the north-western limit of the Gallah Province on the Gascoyne margin (Direen et al. 2008) (Figs 1B and 10B). From the distribution of the magnetic chrons (Fig. 1B), our recognition of a continental chemical signature within the Sonne Ridge basalt (Fig. 9), and the probable sub-aerial or shallow-water elevation of the ridge during extension, make it plausible that full continental lithospheric rupture may not have occurred in the CAP (Fig. 10). Instead, we suggest rupture of the continental lithosphere and onset of seafloor spreading occurred simultaneously offshore the Cuvier and Gascoyne margins at ~131 Ma (Hauterivian), following an oceanwards ridge jump from the Sonja Ridge, producing unambiguous oceanic crust recording chron M5 (Figs 1 and 10) (e.g., Robb et al. 2005; Direen et al. 2008). Continuation of the COTZ across the CAP has implications for the timing and kinematics of plate reconstructions of the NW Australian margin, with the onset of deep-marine seafloor spreading potentially ~3 Myr later than suggested by previous studies (e.g., Robb et al. 2005).

Interpreting the CAP as a COTZ developed through sub-aerial, or at least shallow-water, extension implies its crust was: (i) thicker during SDR emplacement, but concurrently and/or subsequently thinned during continued magmatic extension and late-stage stretching (e.g., Bastow & Keir 2011; Bastow et al. 2018); (ii) less dense and thus more buoyant than 100% oceanic crust, because it likely retained a significant proportion of continental material; and (iii) thermally buoyant due to the presence of abundant hot intrusions and underlying, decompressing mantle. That these processes can maintain rift axes at above or near sea-level elevations is demonstrated by the onshore occurrence of active rift zones, characterised by heavily-intruded continental crust, in the Main Ethiopia Rift and Afar (e.g., Hayward & Ebinger 1996; Ebinger & Casey 2001; Mackenzie et al. 2005; Bridges et al. 2012).

Because the degree of thermal subsidence is at least partly controlled by crustal density, we would expect oceanic crust to thermally subside more than less dense, heavily-intruded continental crust. Given the Hauterivian-to-Middle Barremian sedimentary strata overlying the SDRs were deposited in neritic conditions (Veevers & Johnstone 1974; Holbourn & Kaminski 1995; Oosting et al. 2006), it is apparent the CAP subsided from near sea-level to a current, unloaded basement depth of ~6.5 km; this total subsidence is greater than predicted for dense, thermally subsiding oceanic crust (Stein & Stein 1992). To interpret the CAP as COTZ crust, our results would require other mechanisms, in addition to thermal subsidence, to influence its subsidence history. For example, post-breakup decay of asthenospheric thermal anomalies may account for some elevation discrepancies via removal of dynamic support of the margin (e.g., Czarnota et al. 2013). Finally, the CAP COTZ may have involved some late-stage stretching prior to terminal breakup and the onset of seafloor spreading, akin to processes observed today in the sub-aerial Red Sea rift in Ethiopia (e.g., Bastow & Keir 2011; Daniels et al. 2014).

Development of magnetic stripes during break-up

Recent forward modelling of conjugate, ship-track magnetic profiles by Collier et al. (2017) suggest magnetic signals over SDRs arise from a combination of stacked and rotated lavas, producing a long-wavelength positive anomaly that can sometimes mask reversals, and linear magnetic anomalies caused by dyke intrusion in the underlying crust. Stacked SDR wedges on the CAP are part of a possible COTZ and span several chrons (e.g. M8n-M7r), but are ≤4.5 km thick (Figs 5 and 6). These observations indicate the CAP magnetic stripes likely record magnetic reversal signatures originating from sub-SDR rocks; i.e. the SDRs and flat-lying lavas are too thin to dominate the magnetic signature (cf. Collier et al. 2017). In contrast¸ the less-clearly developed yet higher amplitude magnetic reversals in the Gallah

Province COTZ may relate to interference from the greater SDR thicknesses (≤5.5 km) relative to the CAP (Direen et al. 2008). Our inference that the magnetic signature is derived from sub-SDR rocks is consistent with studies of onshore incipient spreading centres (e.g. Ethiopia), where magnetic stripes likely originate from axial intrusion by dykes in heavily intruded, upper continental crust, rather than overlying lavas (Bridges et al. 2012).

We suggest that SDR thickness and, thereby, preservation of magnetic anomalies within a COTZ can partly be attributed to extension rate. For example, the extension rate during SDR eruption offshore NW Australia (~4.5 cm/yr half rate; Robb et al. 2005) is substantially faster than the inferred extension rates for the South Atlantic during magmatic crust formation (~1.1 cm/yr half-rate; Paton et al. 2017). Slower extension rates (e.g. South Atlantic) likely promote stacking of lava flows to produce thicker SDRs (Eagles et al. 2015), leading to interference between the magnetic signal of the SDRs and sub-SDR crust and thus the development of the long-wavelength positive magnetic anomalies (e.g., Moulin et al. 2010). Extension rate may also influence magnetic anomaly development by affecting the width of magnetic stripes; reversal anomalies will be narrowest at slow spreading ridges (Vine 1966). The narrower anomalies, combined with the greater potential for vertical stacking of lavas, will tend to suppress magnetic anomaly preservation.

Conclusions

The recognition of magnetic stripes within the Cuvier Abyssal Plain (CAP), offshore NW Australia, has led to the assumption that it comprises oceanic crust generated by conventional seafloor spreading at the Sonne Ridge, probably at water depths of ≳2 km. We challenge this assumption, in line with the growing consensus that magnetic stripes are not necessarily diagnostic of oceanic crust and can instead form in continent-ocean transition zones (COTZs). Using regional 2D seismic reflection lines we demonstrate that the uppermost layer in the CAP crystalline line crust contains seaward-dipping reflector (SDR) sequences, akin to those observed in the previously defined COTZ of the Cuvier Margin and Wallaby Saddle, as well as on the heavily intruded continental crust of the Wallaby Plateau. Through comparison to SDRs recognised elsewhere, we suggest those observed across the CAP comprise lavas, interbedded with sedimentary strata, erupted from an axial magmatic segment. Lithological and biostratigraphic data from a borehole penetrating the CAP sedimentary cover, which were deposited in neritic (<200 m water depth) conditions, require the underlying crystalline crust to have been at shallow-water depths ~9 Myr after its formation and thus imply SDR emplacement occurred in a shallow water or sub-aerial environment. We also re-interpret chemical data from a basalt dredged along the Sonne Ridge and, contrary to previous work, show that it exhibits a continental chemical signature. Overall, these data and interpretations suggest the CAP may not comprise unambiguous oceanic crust, but could instead represent a >500 km wide COTZ where extension likely became more magma-dominated, producing heavily-intruded continental crust (akin to present-day Ethiopia) through to magmatic crust. In our model, break-up of the continental crust occurred during the formation of the CAP, but full continental lithospheric rupture occurred outboard of the COTZ following a ridge jump at ~130 Ma. Our re-evaluation of the CAP crustal type supports suggestions that COTZs along volcanic passive margins may record the development of magnetic stripes, which thus should not be used alone as a reliable proxy for the onset of seafloor spreading and the extent of oceanic crust.

Acknowledgements

Schlumberger are thanked for provision of Petrel software licenses. M.T.R. was supported by NERC grant NE/L501621/L. The EW0113 seismic survey and EMAG2 magnetic anomaly grids were, and can be acquired from, the UTIG Marine Geoscience Data System and the

NOAA National Geophysical Data Centre, respectively. Gwenn Peron-Pinvidic, Gareth Roberts, and Saskia Goes are thanked for helpful discussions during the preparation of this manuscript. We thank five reviewers, including Jon Bull, for their constructive comments on previous versions of this manuscript.

Figure captions

Figure 1: (A) Location map of the study area highlighting the seismic lines used in this study and key tectonic elements, including areas of recognised seaward-dipping reflectors (SDRs) (Symonds et al. 1998; Holford et al. 2013) and previously interpreted approximate limits of the continent-ocean boundary (COB; Eagles et al. 2015) and continent-ocean transition zones (COTZs; Symonds et al. 1998; Direen et al. 2008). Inset: study area location offshore NW Australia. AAP – Argo Abyssal Plain, CAP – Cuvier Abyssal Plain, CRFZ – Cape Range Fracture Zone, GAP – Gascoyne Abyssal Plain, GP – Gallah Province, NCB – North Carnarvon Basin, EP – Exmouth Plateau, PB – Perth Basin, SCB – South Carnarvon Basin, Cu – Cuvier margin COTZ, SR – Sonne Ridge, SjR – Sonja Ridge, WP – Wallaby Plateau, WS – Wallaby Saddle, WZFZ – Wallaby-Zenith Fracture Zone. Dredge sites 52, 55 (samples 055BS004A and 055BS004B), and 57 (sample 057DR051A) are also shown (Dadd et al. 2015). (B) Total magnetic intensity grid (EMAG2v2), interpreted magnetic chrons (based on Robb et al. 2005). See Supplementary Figure S1 for an uninterpreted version. (C) Uninterpreted and interpreted seismic line (i.e. seismic profile 670) across the Cuvier Margin, imaging the crustal structure beneath the continental shelf and the deep abyssal plain (modified from Hopper et al., 1992). Velocity profiles from refraction experiments shown; see Hopper et al., (1992) for details. See Figure 1A for approximate line location and Supplementary Figure S2 for an enlarged version of the uninterpreted seismic line.

Figure 2: Schematic model (not to scale) of a continent-ocean transition zone along a magma-rich passive margin, which depicts the evolution from unambiguous continental crust to unambiguous oceanic crust; for simplicity the lithospheric mantle is not shown. As magma intrudes continental crust, likely as dykes at mid- to upper-crustal levels and larger gabbroic bodies in the lower crust, it becomes ‘heavily intruded continental crust’ (e.g., Eldholm et al. 1989). Continued intrusion and dyking leads to localisation of magmatism within narrow zones where there is little, if any, continental crust remaining (i.e. 'magmatic crust'; e.g., Collier et al. 2017; Paton et al. 2017). We categorize heavily intruded continental crust and magmatic crust as ‘COTZ crust’. Sub-aerial, magma-assisted rifting may feed extensive lava flows that later, through subsidence, become seaward-dipping reflectors (SDRs). SDR subsidence leads to rotation of underlying dykes (Abdelmalak et al. 2015); a similar rotation of lavas and dykes is observed in oceanic crust (Karson 2019).

Figure 3: Tectono-stratigraphic chart for the Exmouth Plateau and Cuvier Margin (after Hocking et al., 1987; Arditto, 1993; Partington et al. 2003; Willis, 2005; Reeve et al. 2016). (B) Comparison between stratigraphic data from DSDP 263 and Pendock-1 boreholes (modified from Veevers & Johnstone, 1974; Holbourn & Kaminski, 1995). See Figure 1A for borehole locations.

Figure 4: Total magnetic intensity grids EMAG2v2 and EMAG2v3 (Maus et al. 2009; Meyer et al. 2017), compared with shiptrack magnetic data (Robb et al. 2005). Key tectonic elements also shown (see Fig. 1 for legend). In (A), CAP – Cuvier Abyssal Plain, GAP – Gascoyne Abyssal Plain, GP – Gallah Province, NCB – North Carnarvon Basin, PB – Perth Basin, SCB – South Carnarvon Basin, Cu – Cuvier margin COTZ, WP – Wallaby Plateau, WS – Wallaby Saddle.

Figure 5: Interpreted and uninterpreted, depth-converted seismic lines (A) EW0113-5 and (B) EW0113-6, and the time-migrated line (D) repro n303 showing crustal structure of the Cuvier Margin; see Figures 1A and 5C for line locations. The tie-co-located magnetic anomaly profile showing interpreted magnetic chrons is presented for (A–D) (after Robb et al. 2005). See Supplementary Figure S2 for an enlarged version of the uninterpreted seismic lines.

Figure 6: Zoomed in view of EW0113-5 highlighting the seismic character of interpreted SDR packages (see Fig. 5A for location).

Figure 7: Interpreted and uninterpreted, time-migrated seismic line s135-11; see Figure 1A for location. See Supplementary Figure S2 for an enlarged version of the uninterpreted seismic line.

Figure 8: Interpreted and uninterpreted, time-migrated seismic lines (A) s135-s135_05, (B) s135-08, and (D) s310-59 showing crustal structure of the Wallaby Plateau and Wallaby Saddle; see Figures 1A and 8D for line locations. See Supplementary Figure S2 for an enlarged version of the uninterpreted seismic lines.

Figure 9: (A) Primitive mantle normalized incompatible element diagram comparing the dredged Sonne Ridge and Wallaby Plateau basalt lava samples with average (ave.) compositions of MORB variants (Hofmann 2014), Globally Subducting Sediment (GLOSS) (Plank & Langmuir 1998), and continental crust (Rudnick & Fountain 1995). (B) Plot of ε(Nd) versus $^{87}Sr/^{86}Sr$, illustrating that the Sonne Ridge and Wallaby Plateau samples are distinct from MORB (based on data collated in Hofmann 2014).

Figure 10: (A) Map showing the potential limits of the COTZ based on interpreting the CAP and Gallah Province as transitional and/or magmatic crust. (B-D) Schematic maps showing the development of COTZ crust and the onset of oceanic crust accretion adjacent to the Gascoyne and Cuvier margins, during formation of chrons (B) M10, (C) M6 and (D) M3r. See Figure 1 for chron ages. Location of present day coastline shown for reference.

References

Abdelmalak, M.M., Andersen, T.B., Planke, S., Faleide, J.I., Corfu, F., Tegner, C., Shephard, G.E., Zastrozhnov, D., *et al.* 2015. The ocean-continent transition in the mid-Norwegian margin: Insight from seismic data and an onshore Caledonian field analogue. *Geology*, **43**, 1011-1014.

Bastow, I.D. & Keir, D. 2011. The protracted development of the continent-ocean transition in Afar. *Nature Geosci*, **4**, 248-250.

Bastow, I.D., Booth, A.D., Corti, G., Keir, D., Magee, C., Jackson, C.A.L., Warren, J., Wilkinson, J., *et al.* 2018. The Development of Late-Stage Continental Breakup: Seismic Reflection and Borehole Evidence from the Danakil Depression, Ethiopia. **37**, 2848-2862.

Bodvarsson, G. & Walker, G. 1964. Crustal drift in Iceland. *Geophysical Journal International*, **8**, 285-300.

Bolli, H.M. 1974. *Jurassic and Cretaceous Calcisphaerulidae from DSDP Leg 27, eastern Indian Ocean*.

Bridges, D.L., Mickus, K., Gao, S.S., Abdelsalam, M.G. & Alemu, A. 2012. Magnetic stripes of a transitional continental rift in Afar. *Geology*, **40**, 203-206.

Bronner, A., Sauter, D., Manatschal, G., Péron-Pinvidic, G. & Munschy, M. 2011. Magmatic breakup as an explanation for magnetic anomalies at magma-poor rifted margins. *Nature Geoscience*, **4**, 549.

Causer, A., Pérez-Díaz, L., Adam, J. & Eagles, G. 2020. Uncertainties in break-up markers along the Iberia–Newfoundland margins illustrated by new seismic data. *Solid Earth*, **11**, 397-417.

Collier, J.S., McDermott, C., Warner, G., Gyori, N., Schnabel, M., McDermott, K. & Horn, B.W. 2017. New constraints on the age and style of continental breakup in the South Atlantic from magnetic anomaly data. *Earth and Planetary Science Letters*, **477**, 27-40.

Colwell, J., Symonds, P. & Crawford, A. 1994. The nature of the Wallaby (Cuvier) Plateau and other igneous provines of the west Australian margin. *Journal of Australian Geology and Geophysics*, **15**, 137-156.

Compton, J., Mallinson, D., Netranatawong, T. & Locker, D. 1992. *Regional correlation of mineralogy and diagenesis of sediment from the Exmouth Plateau and Argo Basin, Northwestern Australian Continental Margin*.

Corti, G., Agostini, A., Keir, D., Van Wijk, J., Bastow, I.D. & Ranalli, G. 2015. Magma-induced axial subsidence during final-stage rifting: Implications for the development of seaward-dipping reflectors. *Geosphere*, **11**, 563-571.

Crawford, A.J. & von Rad, U. 1994. The petrology, geochemistry and implications of basalts dredged from the Rowley Terrace-Scott Plateau and Exmouth Plateau margins, northwestern Australia. *Journal of Australian Geology and Geophysics*, **15**, 43-54.

Czarnota, K., Hoggard, M., White, N. & Winterbourne, J. 2013. Spatial and temporal patterns of Cenozoic dynamic topography around Australia. *Geochemistry, Geophysics, Geosystems*, **14**, 634-658.

Dadd, K.A., Kellerson, L., Borissova, I. & Nelson, G. 2015. Multiple sources for volcanic rocks dredged from the Western Australian rifted margin. *Marine Geology*, **368**, 42-57.

Daniell, J., Jorgensen, D., Anderson, T., Borissova, I., Burq, S., Heap, A., Hughes, D., Mantle, D., *et al.* 2009. Frontier basins of the West Australian continental margin. *Geoscience Australia Record*, **38**, 243.

Daniels, K.A., Bastow, I.D., Keir, D., Sparks, R.S.J. & Menand, T. 2014. Thermal models of dyke intrusion during development of continent–ocean transition. *Earth and Planetary Science Letters*, **385**, 145-153.

Direen, N.G., Stagg, H.M.J., Symonds, P.A. & Colwell, J.B. 2008. Architecture of volcanic rifted margins: new insights from the Exmouth – Gascoyne margin, Western Australia. *Australian Journal of Earth Sciences*, **55**, 341-363.

Direen, N.G., Borissova, I., Stagg, H., Colwell, J.B. & Symonds, P.A. 2007. Nature of the continent–ocean transition zone along the southern Australian continental margin: a comparison of the Naturaliste Plateau, SW Australia, and the central Great Australian Bight sectors. *Geological Society, London, Special Publications*, **282**, 239-263.

Eagles, G., Pérez-Díaz, L. & Scarselli, N. 2015. Getting over continent ocean boundaries. *Earth-Science Reviews*, **151**, 244-265.

Ebinger, C.J. & Casey, M. 2001. Continental breakup in magmatic provinces: An Ethiopian example. *Geology*, **29**, 527.

Eittreim, S.L., Gnibidenko, H., Helsley, C.E., Sliter, R., Mann, D. & Ragozin, N. 1994. Oceanic crustal thickness and seismic character along a central Pacific transect. *Journal of Geophysical Research: Solid Earth*, **99**, 3139-3145.

Eldholm, O., Thiede, J. & Taylor, E. 1989. The Norwegian continental margin: tectonic, volcanic, and paleoenvironmental framework. *Proceedings of the ocean drilling program, Scientific results*. Citeseer, 5-26.

Eldholm, O., Thiede, J., Taylor, E. & Party, S.S. 1987. Summary and preliminary conclusions, ODP Leg 104. *Proceedings of the Ocean Drilling Program, Scientific Results*. Ocean Drilling Program College Station, Texas, 751-771.

Falvey, D. & Veevers, J. 1974. Physiography of the Exmouth and Scott plateaus, western Australia, and adjacent northeast Wharton Basin. *Marine Geology*, **17**, 21-59.

Geoffroy, L., Callot, J.P., Scaillet, S., Skuce, A., Gélard, J., Ravilly, M., Angelier, J., Bonin, B., *et al.* 2001. Southeast Baffin volcanic margin and the North American-Greenland plate separation. *Tectonics*, **20**, 566-584.

Gibbons, A.D., Barckhausen, U., den Bogaard, P., Hoernle, K., Werner, R., Whittaker, J.M. & Müller, R.D. 2012. Constraining the Jurassic extent of Greater India: Tectonic evolution of the West Australian margin. *Geochemistry, Geophysics, Geosystems*, **13**.

Goncharov, A. & Nelson, G. 2012. From two way time to depth and pressure for interpretation of seismic velocities offshore: Methodology and examples from the Wallaby Plateau on the West Australian margin. *Tectonophysics*, **572**, 26-37.

Gradstein, F. & Ogg, J. 2012. The chronostratigraphic scale *The geologic time scale*. Elsevier, 31-42.

Harkin, C., Kusznir, N., Roberts, A., Manatschal, G. & Horn, B. 2020. Origin, composition and relative timing of seaward dipping reflectors on the Pelotas rifted margin. *Marine and petroleum geology*, **114**, 104235.

Hayward, N. & Ebinger, C. 1996. Variations in the along-axis segmentation of the Afar Rift system. *Tectonics*, **15**, 244-257.

Heine, C. & Müller, R. 2005. Late Jurassic rifting along the Australian North West Shelf: margin geometry and spreading ridge configuration. *Australian Journal of Earth Sciences*, **52**, 27-39.

Hey, R. 1977. A new class of “pseudofaults” and their bearing on plate tectonics: A propagating rift model. *Earth and Planetary Science Letters*, **37**, 321-325.

Hinz, K. 1981. A hypothesis on terrestrial catastrophies Wedges of very thick oceanward dipping layers beneath passive continental margins. Their origin and paleoenvironmental significance. *Geologisches Jahrbuch. Reihe E, Geophysik*, 3-28.

Hofmann, A. 2014. Sampling mantle heterogeneity through oceanic basalts: Isotopes and trace elements. *In*: RW, C. (ed) *The Mantle and Core, Treatise on Geochemistry*. Elsevier-Pergamon, Oxford, 67-101.

Holbourn, A.E. & Kaminski, M.A. 1995. Lower Cretaceous benthic foraminifera from DSDP Site 263: micropalaeontological constraints for the early evolution of the Indian Ocean. *Marine Micropaleontology*, **26**, 425-460.

Holford, S.P., Schofield, N., Jackson, C.A.L., Magee, C., Green, P.F. & Duddy, I.R. 2013. Impacts of igneous intrusions on source and reservoir potential in prospective sedimentary basins along the western Australian continental margin. *In*: Keep, M. & Moss, S.J. (eds) *The Sedimentary Basins of Western Australia IV*. Proceedings of the Petroleum Exploration Society of Australia Symposium, Perth, WA.

Hopper, J.R., Mutter, J.C., Larson, R.L. & Mutter, C.Z. 1992. Magmatism and rift margin evolution: Evidence from northwest Australia. *Geology*, **20**, 853-857.

Karson, J.A. 2019. From Ophiolites to Oceanic Crust: Sheeted Dike Complexes and Seafloor Spreading. *In*: Srivastava, R., Ernst, R. & Peng, P. (eds) *Dyke Swarms of the World: A Modern Perspective*. Springer, 459-492.

Keranen, K., Klemperer, S., Gloaguen, R. & Group, E.W. 2004. Three-dimensional seismic imaging of a protoridge axis in the Main Ethiopian rift. *Geology*, **32**, 949-952.

Larsen, H. & Saunders, A. 1998. 41. Tectonism and volcanism at the Southeast Greenland rifted margin: a record of plume impact and later continental rupture. *Proceedings of the Ocean Drilling Program, Scientific Results*, 503-533.

Larsen, H., Saunders, A. & Clift, P. 1994a. Proceedings of the Ocean Drilling Program, Initial Reports. *Ocean Drilling Program*, College Station, Texas, 1-152.

Larsen, H., Saunders, A., Larsen, L. & Lykke-Andersen, H. 1994b. ODP activities on the South-East Greenland margin: Leg 152 drilling and continued site surveying. *Rapport Grønlands Geologiske Undersøgelse*, **160**, 75-81.

Larson, R.L., Mutter, J.C., Diebold, J.B., Carpenter, G.B. & Symonds, P. 1979. Cuvier Basin: a product of ocean crust formation by Early Cretaceous rifting off Western Australia. *Earth and Planetary Science Letters*, **45**, 105-114.

Lenoir, X., Féraud, G. & Geoffroy, L. 2003. High-rate flexure of the East Greenland volcanic margin: constraints from 40Ar/39Ar dating of basaltic dykes. *Earth and Planetary Science Letters*, **214**, 515-528.

Longley, I., Buessenschuett, C., Clydsdale, L., Cubitt, C., Davis, R., Johnson, M., Marshall, N., Murray, A., *et al.* 2002. The North West Shelf of Australia–a Woodside perspective. *The sedimentary basins of Western Australia*, **3**, 27-88.

Mackenzie, G., Thybo, H. & Maguire, P. 2005. Crustal velocity structure across the Main Ethiopian Rift: results from two-dimensional wide-angle seismic modelling. *Geophysical Journal International*, **162**, 994-1006.

MacLeod, S.J., Williams, S.E., Matthews, K.J., Müller, R.D. & Qin, X. 2017. A global review and digital database of large-scale extinct spreading centers. *Geosphere*, **13**, 911-949.

Maguire, P., Keller, G., Klemperer, S., Mackenzie, G., Keranen, K., Harder, S., O Reilly, B., Thybo, H., *et al.* 2006. Crustal structure of the northern Main Ethiopian Rift from the EAGLE controlled-source survey; a snapshot of incipient lithospheric break-up. *Geological Society, London, Special Publications*, **259**, 269.

Maus, S., Barckhausen, U., Berkenbosch, H., Bournas, N., Brozena, J., Childers, V., Dostaler, F., Fairhead, J., *et al.* 2009. EMAG2: A 2–arc min resolution Earth Magnetic Anomaly Grid compiled from satellite, airborne, and marine magnetic measurements. *Geochemistry, Geophysics, Geosystems*, **10**.

McDermott, C., Lonergan, L., Collier, J.S., McDermott, K.G. & Bellingham, P. 2018. Characterization of Seaward-Dipping Reflectors Along the South American Atlantic Margin and Implications for Continental Breakup. *Tectonics*, **37**, 3303-3327.

McDermott, C., Collier, J.S., Lonergan, L., Fruehn, J. & Bellingham, P. 2019. Seismic velocity structure of seaward-dipping reflectors on the South American continental margin. *Earth and Planetary Science Letters*, **521**, 14-24.

Menard, H. 1969. Elevation and subsidence of oceanic crust. *Earth and Planetary Science Letters*, **6**, 275-284.

Menzies, M., Klemperer, S., Ebinger, C. & Baker, J. 2002. Characteristics of volcanic rifted margins. *In*: Menzies, M., Klemperer, S., Ebinger, C. & Baker, J. (eds) *Volcanic Rifted Margins, Special Publications*. Geological Society of America, **362**, 1-14.

Meyer, B., Chulliat, A. & Saltus, R. 2017. Derivation and error analysis of the Earth Magnetic Anomaly Grid at 2 arc min Resolution Version 3 (EMAG2v3). *Geochemistry, Geophysics, Geosystems*, **18**, 4522-4537.

Mihut, D. & Müller, R.D. 1998. Volcanic margin formation and Mesozoic rift propagators in the Cuvier Abyssal Plain off Western Australia. *Journal of Geophysical Research*, **103**, 27149.

Moulin, M., Aslanian, D. & Unternehr, P. 2010. A new starting point for the South and Equatorial Atlantic Ocean. *Earth-Science Reviews*, **98**, 1-37.

Mutter, J.C., Talwani, M. & Stoffa, P.L. 1982. Origin of seaward-dipping reflectors in oceanic crust off the Norwegian margin by "subaerial sea-floor spreading". *Geology*, **10**, 353-357.

Norcliffe, J.R., Paton, D.A., Mortimer, E.J., McCaig, A.M., Nicholls, H., Rodriguez, K., Hodgson, N. & Van Der Spuy, D. 2018. Laterally Confined Volcanic Successions (LCVS); recording rift-jumps during the formation of magma-rich margins. *Earth and Planetary Science Letters*, **504**, 53-63.

Olierook, H.K., Merle, R.E., Jourdan, F., Sircombe, K., Fraser, G., Timms, N.E., Nelson, G., Dadd, K.A., *et al.* 2015. Age and geochemistry of magmatism on the oceanic Wallaby Plateau and implications for the opening of the Indian Ocean. *Geology*, **43**, 971-974.

Oosting, A., Leereveld, H., Dickens, G., Henderson, R. & Brinkhuis, H. 2006. Correlation of Barremian-Aptian (mid-Cretaceous) dinoflagellate cyst assemblages between the Tethyan and Austral realms. *Cretaceous Research*, **27**, 792-813.

Parsons, B. & Sclater, J.G. 1977. An analysis of the variation of ocean floor bathymetry and heat flow with age. *Journal of Geophysical Research*, **82**, 803-827.

Paton, D., Pindell, J., McDermott, K., Bellingham, P. & Horn, B. 2017. Evolution of seaward-dipping reflectors at the onset of oceanic crust formation at volcanic passive margins: Insights from the South Atlantic. *Geology*, **45**, 439-442.

Peron-Pinvidic, G., Manatschal, G. & Participants, a.t.I.R.W. 2019. Rifted margins: state of the art and future challenges. *Frontiers in Earth Science*, **7**, 8.

Phipps-Morgan, J. & Chen, Y.J. 1993. The genesis of oceanic crust: Magma injection, hydrothermal circulation, and crustal flow. *Journal of Geophysical Research: Solid Earth*, **98**, 6283-6297.

Pickup, S., Whitmarsh, R., Fowler, C. & Reston, T. 1996. Insight into the nature of the ocean-continent transition off West Iberia from a deep multichannel seismic reflection profile. *Geology*, **24**, 1079-1082.

Plank, T. & Langmuir, C.H. 1998. The chemical composition of subducting sediment and its consequences for the crust and mantle. *Chemical Geology*, **145**, 325-394.

Planke, S. & Eldholm, O. 1994. Seismic response and construction of seaward dipping wedges of flood basalts: Vøring volcanic margin. *Journal of Geophysical Research: Solid Earth*, **99**, 9263-9278.

Planke, S., Symonds, P.A., Alvestad, E. & Skogseid, J. 2000. Seismic volcanostratigraphy of large-volume basaltic extrusive complexes on rifted margins. *Journal of Geophysical Research: Solid Earth*, **105**, 19335-19351.

Rabinowitz, P.D. & LaBrecque, J. 1979. The Mesozoic South Atlantic Ocean and evolution of its continental margins. *Journal of Geophysical Research: Solid Earth*, **84**, 5973-6002.

Robb, M.S., Taylor, B. & Goodliffe, A.M. 2005. Re-examination of the magnetic lineations of the Gascoyne and Cuvier Abyssal Plains, off NW Australia. *Geophysical Journal International*, **163**, 42-55.

Roberts, D., Backman, J., Morton, A., Murray, J. & Keene, J. 1984. *Evolution of volcanic rifted margins – synthesis of leg-81 results on the West margin of Rockall Plateau*.

Robinson, P.T., Thayer, P., Cook, P., McKnight, B. & et al. 1974. *Lithology of Mesozoic and Cenozoic sediments of the eastern Indian Ocean, Leg 27, Deep Sea Drilling Project*.

Rooney, T.O., Bastow, I.D., Keir, D., Mazzarini, F., Movsesian, E., Grosfils, E.B., Zimbelman, J.R., Ramsey, M.S., *et al.* 2014. The protracted development of focused magmatic intrusion during continental rifting. *Tectonics*, **33**, 875-897.

Rudnick, R.L. & Fountain, D.M. 1995. Nature and composition of the continental crust: a lower crustal perspective. *Reviews of Geophysics*, **33**, 267-309.

Sayers, J., Borissova, I., Ramsay, D. & Symonds, P. 2002. *Geological framework of the Wallaby Plateau and adjacent areas*.

Scheibnerová, V. 1974. *Aptian–Albian benthonic foraminifera from DSDP Leg 27, Sites 259, 260 and 263, Eastern Indian Ocean*.

Skogseid, J., Pedersen, T., Eldholm, O. & Larsen, B.T. 1992. Tectonism and magmatism during NE Atlantic continental break-up: the Voring Margin. *Geological Society, London, Special Publications*, **68**, 305-320.

Skogseid, J., Planke, S., Faleide, J.I., Pedersen, T., Eldholm, O. & Neverdal, F. 2000. NE Atlantic continental rifting and volcanic margin formation. *In*: Nottvedt, A. (ed) *Dynamics of the Norwegian Margin*. Geological Society, London, Special Publications, London, **167**, 295-326.

Stagg, H., Alcock, M., Bernardel, G., Moore, A., Symonds, P. & Exon, N. 2004. *Geological framework of the outer Exmouth Plateau and adjacent ocean basins*. Geoscience Australia.

Stein, C.A. & Stein, S. 1992. A model for the global variation in oceanic depth and heat flow with lithospheric age. *Nature*, **359**, 123.

Stilwell, J., Quilty, P. & Mantle, D. 2012. Paleontology of Early Cretaceous deep-water samples dredged from the Wallaby Plateau: new perspectives of Gondwana break-up along the Western Australian margin. *Australian Journal of Earth Sciences*, **59**, 29-49.

Symonds, P.A., Planke, S., Frey, O. & Skogseid, J. 1998. Volcanic evolution of the Western Australian Continental Margin and its implications for basin development. *The Sedimentary Basins of Western Australia 2: Proc. of Petroleum Society Australia Symposium, Perth, WA.*

Talwani, M. & Eldholm, O. 1973. Boundary between continental and oceanic crust at the margin of rifted continents. *Nature*, **241**, 325.

Tian, X. & Buck, W.R. 2019. Lithospheric thickness of volcanic rifting margins: Constraints from seaward dipping reflectors. *Journal of Geophysical Research: Solid Earth*, **124**, 3254-3270.

Tischer, M. 2006. *The structure and development of the continent-ocean transition zone of the Exmouth Plateau and Cuvier margin, Northwest Australia: implications for extensional strain partitioning.* PhD, Columbia University.

Veevers, J. 1986. Breakup of Australia and Antarctica estimated as mid-Cretaceous (95±5 Ma) from magnetic and seismic data at the continental margin. *Earth and Planetary Science Letters*, **77**, 91-99.

Veevers, J. & Johnstone, M. 1974. Comparative stratigraphy and structure of the western Australian margin and the adjacent deep ocean floor. *Initial Reports of the Deep Sea Drilling Project*, **27**, 571-585.

Vine, F.J. 1966. Spreading of the ocean floor: new evidence. *Science*, **154**, 1405-1415.

Vine, F.J. & Matthews, D.H. 1963. Magnetic anomalies over oceanic ridges. *Nature*, **199**, 947-949.

Wiseman, J.F. & Williams, A. 1974. *Palynological investigation of samples from sites 259, 261, and 263, Leg 27, Deep Sea Drilling Project*.

Table 1: Interval velocities

Layer	Seismic velocity (km s^{-1})
Water column	1.5
Sedimentary strata	2.0–2.8
Seaward-dipping reflectors (SDRs)	4.9
Sub-SDR crust	6.8–7.2
Upper mantle	8

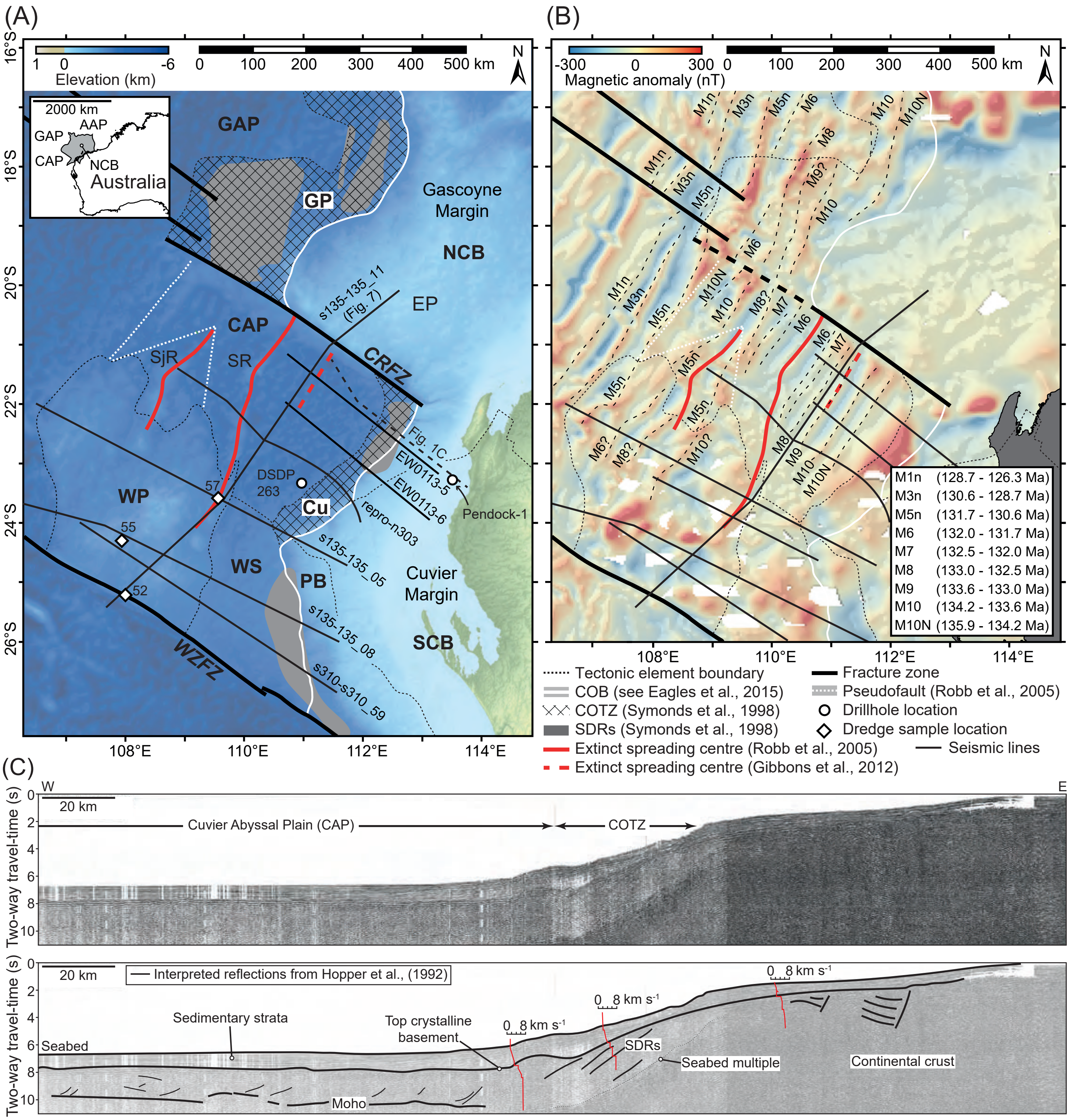
(A)
(B)
(C)
Elevation (km)
Magnetic anomaly (nT)
500 km
GAP
GP
Gascoyne Margin
NCB
CAP
EP
CRFZ
SjR
SR
WP
DSDP 263
Cu
Pendock-1
WS
PB
Cuvier Margin
SCB
WZFZ
Australia
s135-135_11 (Fig. 7)
Fig. 1C
EW0113-5
EW0113-6
repro-n303
s135-135_05
s135-135_08
s310-s310_59
M1n (128.7 - 126.3 Ma)
M3n (130.6 - 128.7 Ma)
M5n (131.7 - 130.6 Ma)
M6 (132.0 - 131.7 Ma)
M7 (132.5 - 132.0 Ma)
M8 (133.0 - 132.5 Ma)
M9 (133.6 - 133.0 Ma)
M10 (134.2 - 133.6 Ma)
M10N (135.9 - 134.2 Ma)
Tectonic element boundary
COB (see Eagles et al., 2015)
COTZ (Symonds et al., 1998)
SDRs (Symonds et al., 1998)
Extinct spreading centre (Robb et al., 2005)
Extinct spreading centre (Gibbons et al., 2012)
Fracture zone
Pseudofault (Robb et al., 2005)
Drillhole location
Dredge sample location
Seismic lines
Two-way travel-time (s)
Cuvier Abyssal Plain (CAP)
COTZ
Interpreted reflections from Hopper et al., (1992)
Sedimentary strata
Seabed
Top crystalline basement
SDRs
Seabed multiple
Continental crust
Moho

Figure 2

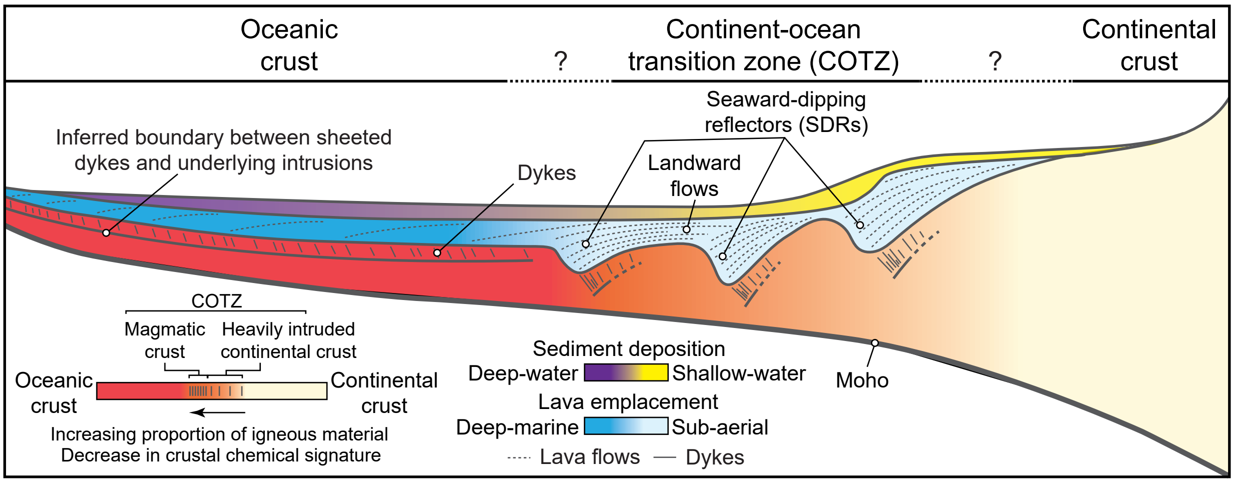

Oceanic crust
?
Continent-ocean transition zone (COTZ)
?
Continental crust
Seaward-dipping reflectors (SDRs)
Inferred boundary between sheeted dykes and underlying intrusions
Dykes
Landward flows
Moho
COTZ
Magmatic crust
Heavily intruded continental crust
Oceanic crust
Continental crust
Increasing proportion of igneous material
Decrease in crustal chemical signature
Sediment deposition
Deep-water
Shallow-water
Lava emplacement
Deep-marine
Sub-aerial
Lava flows
Dykes

Figure 3

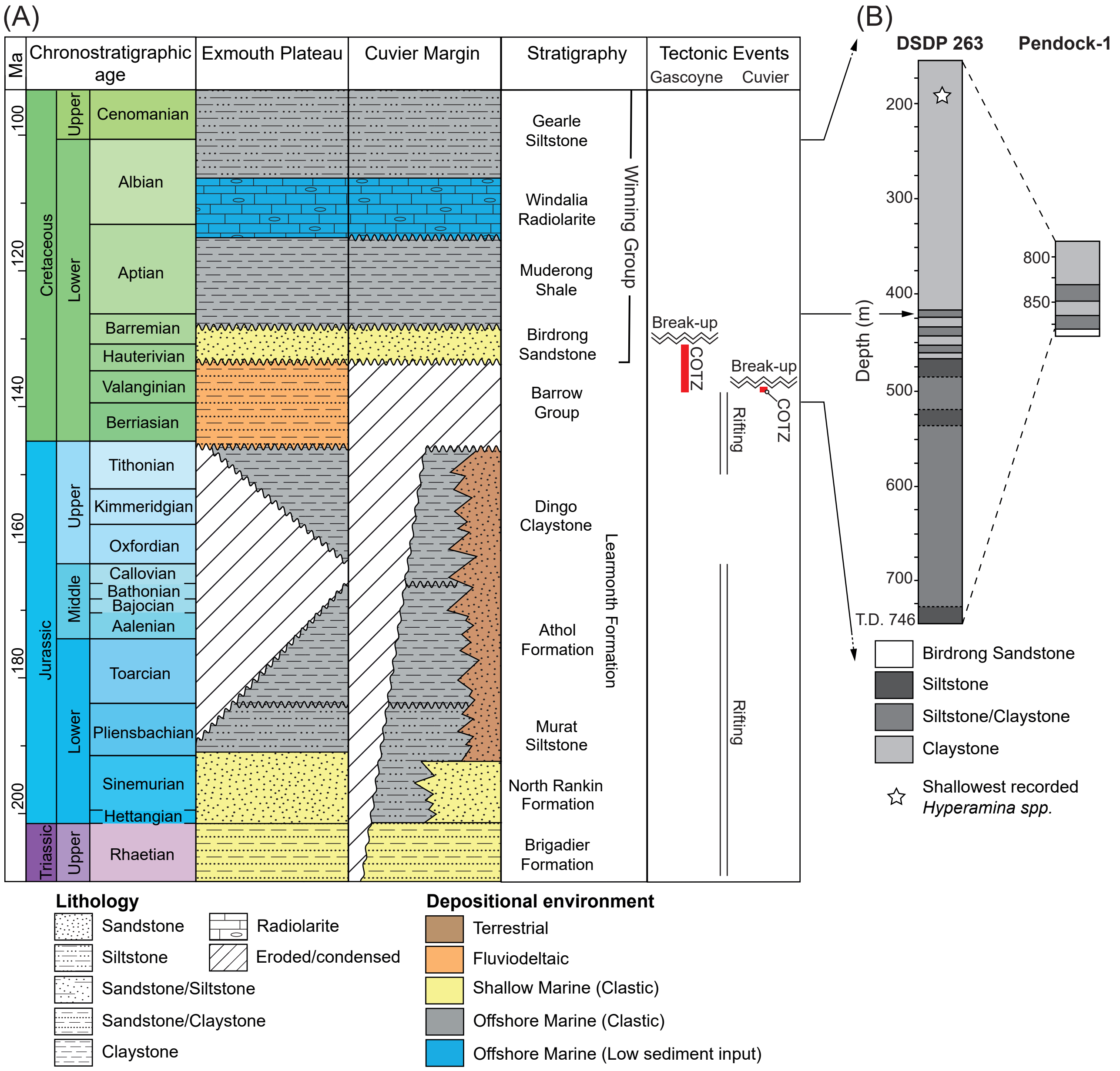

(A)
Ma
Chronostratigraphic age
Exmouth Plateau
Cuvier Margin
Stratigraphy
Tectonic Events
Gascoyne
Cuvier
100
120
140
160
180
200
Cretaceous
Jurassic
Triassic
Upper
Lower
Middle
Cenomanian
Albian
Aptian
Barremian
Hauterivian
Valanginian
Berriasian
Tithonian
Kimmeridgian
Oxfordian
Callovian
Bathonian
Bajocian
Aalenian
Toarcian
Pliensbachian
Sinemurian
Hettangian
Rhaetian
Gearle Siltstone
Windalia Radiolarite
Muderong Shale
Birdrong Sandstone
Barrow Group
Dingo Claystone
Athol Formation
Murat Siltstone
North Rankin Formation
Brigadier Formation
Winning Group
Learmonth Formation
Break-up
COTZ
Rifting
Lithology
Sandstone
Siltstone
Sandstone/Siltstone
Sandstone/Claystone
Claystone
Radiolarite
Eroded/condensed
Depositional environment
Terrestrial
Fluviodeltaic
Shallow Marine (Clastic)
Offshore Marine (Clastic)
Offshore Marine (Low sediment input)
(B)
DSDP 263
Pendock-1
Depth (m)
200
300
400
500
600
700
T.D. 746
800
850
Birdrong Sandstone
Siltstone
Siltstone/Claystone
Claystone
Shallowest recorded *Hyperamina spp.*

Figure 4

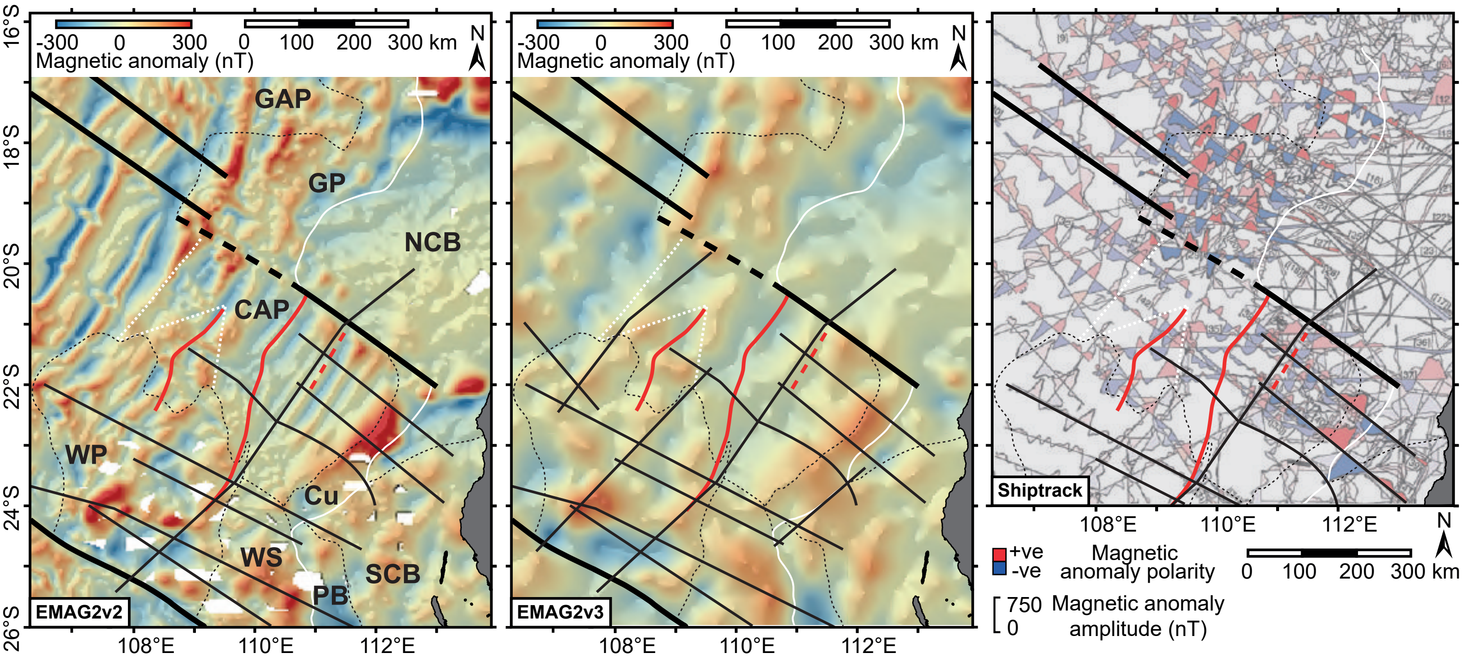
-300 0 300
Magnetic anomaly (nT)
0 100 200 300 km
N
GAP
GP
NCB
CAP
WP
Cu
WS
SCB
PB
EMAG2v2
EMAG2v3
Shiptrack
16°S
18°S
20°S
22°S
24°S
26°S
108°E
110°E
112°E
+ve
-ve
Magnetic anomaly polarity
750
0
Magnetic anomaly amplitude (nT)

Figure 5

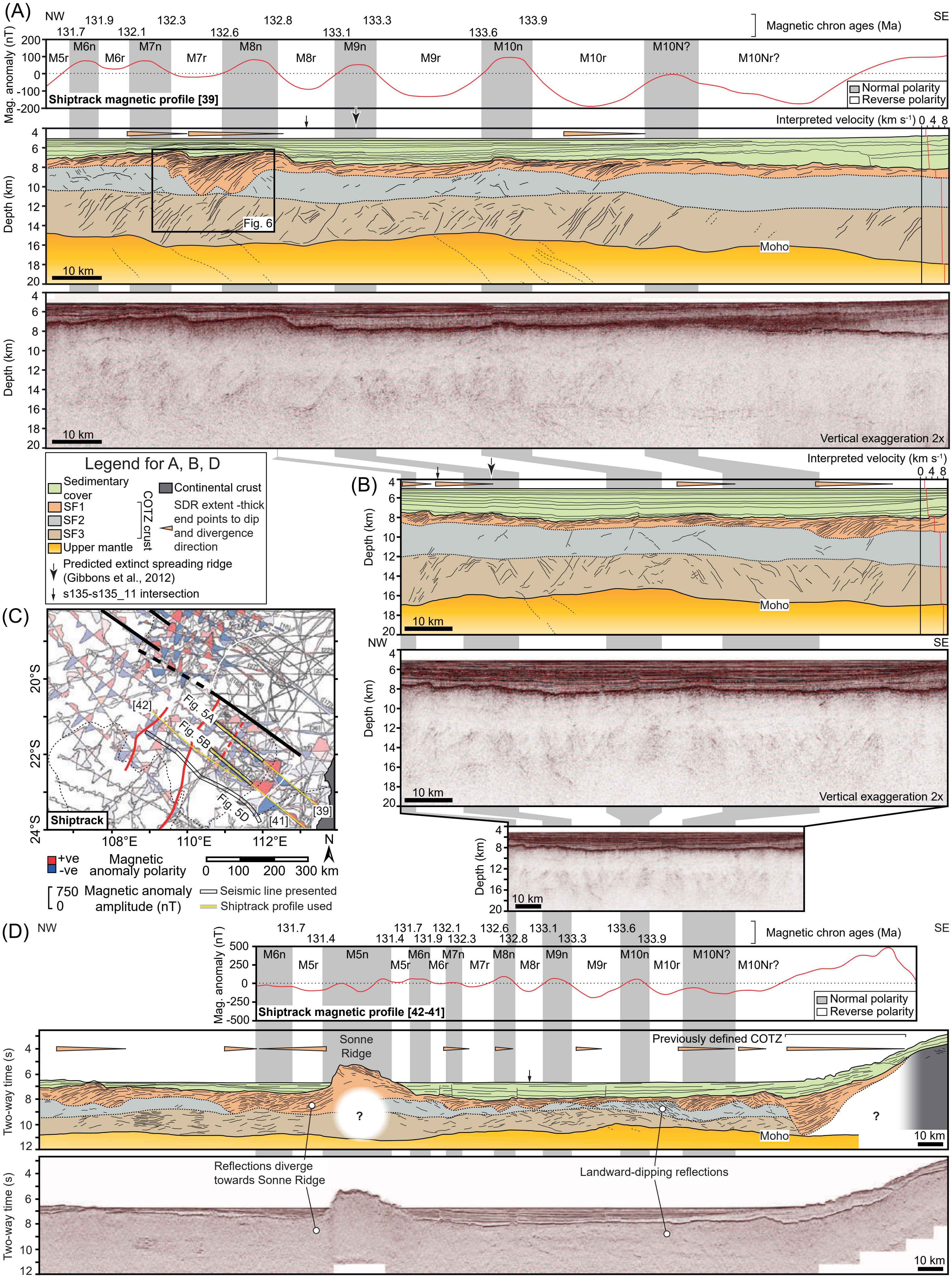

(A)
NW
SE
Magnetic chron ages (Ma)
131.7 131.9 132.1 132.3 132.6 132.8 133.1 133.3 133.6 133.9
M5r M6n M6r M7n M7r M8n M8r M9n M9r M10n M10r M10N? M10Nr?
Mag. anomaly (nT)
Shiptrack magnetic profile [39]
Normal polarity
Reverse polarity
Interpreted velocity (km s-1) 0 4 8
Depth (km)
Fig. 6
Moho
10 km
Vertical exaggeration 2x
Legend for A, B, D
Sedimentary cover
SF1
SF2
SF3
Upper mantle
COTZ crust
Continental crust
SDR extent -thick end points to dip and divergence direction
Predicted extinct spreading ridge (Gibbons et al., 2012)
s135-s135_11 intersection
(B)
(C)
20°S
22°S
24°S
108°E
110°E
112°E
[42]
Fig. 5A
Fig. 5B
Fig. 5D
[39]
[41]
Shiptrack
N
+ve
-ve
Magnetic anomaly polarity
0 100 200 300 km
750
0
Magnetic anomaly amplitude (nT)
Seismic line presented
Shiptrack profile used
(D)
131.7 131.4 131.4 131.7 131.9 132.1 132.3 132.6 132.8 133.1 133.3 133.6 133.9
M6n M5r M5n M5r M6n M6r M7n M7r M8n M8r M9n M9r M10n M10r M10N? M10Nr?
Shiptrack magnetic profile [42-41]
Two-way time (s)
Sonne Ridge
Previously defined COTZ
Reflections diverge towards Sonne Ridge
Landward-dipping reflections

Figure 6

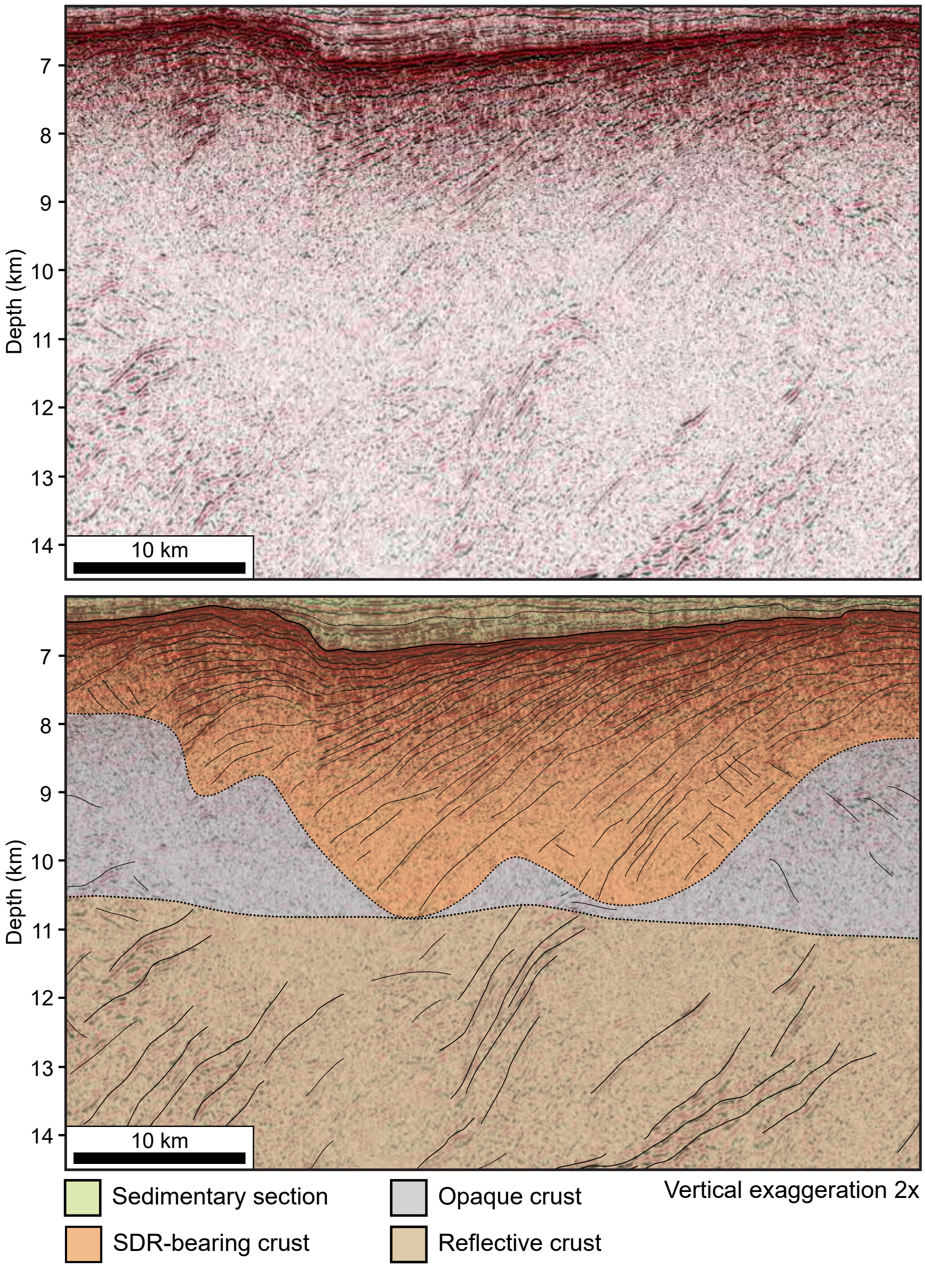

7
8
9
10
11
12
13
14
Depth (km)
10 km
7
8
9
10
11
12
13
14
Depth (km)
10 km
Vertical exaggeration 2x
Sedimentary section
SDR-bearing crust
Opaque crust
Reflective crust

Figure 7

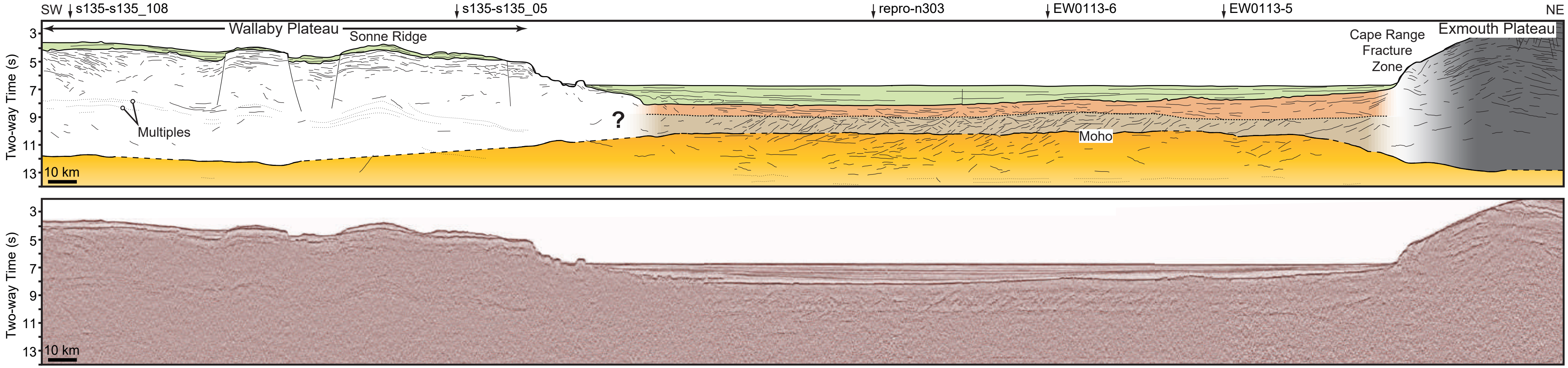
SW
s135-s135_108
s135-s135_05
repro-n303
EW0113-6
EW0113-5
NE
Wallaby Plateau
Sonne Ridge
Cape Range
Fracture
Zone
Exmouth Plateau
?
Multiples
Moho
Two-way Time (s)
3
5
7
9
11
13
10 km
Two-way Time (s)
3
5
7
9
11
13
10 km

Figure 8

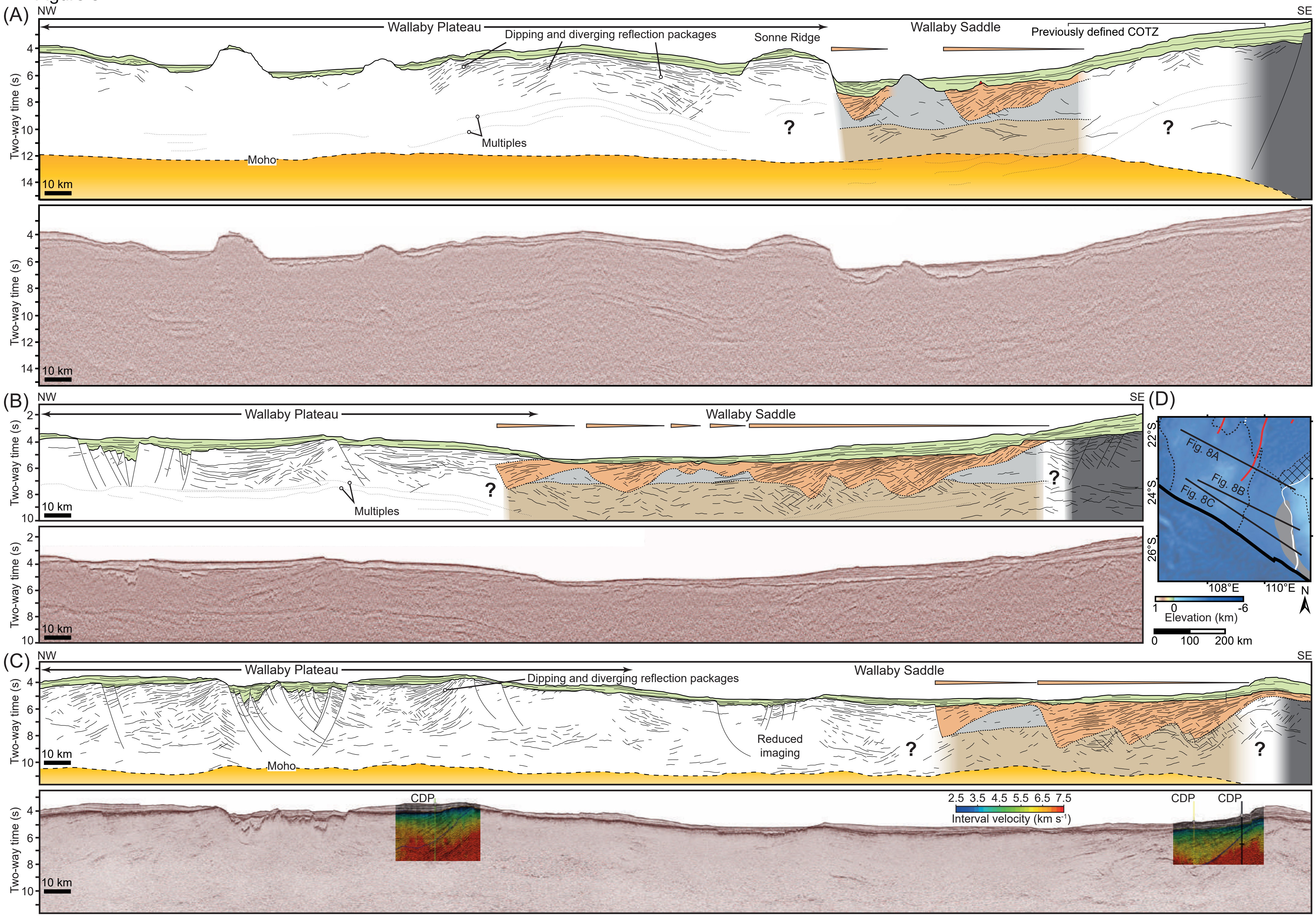

(A)
NW
SE
Wallaby Plateau
Dipping and diverging reflection packages
Sonne Ridge
Wallaby Saddle
Previously defined COTZ
Multiples
Moho
?
Two-way time (s)
10 km
(B)
Wallaby Plateau
Wallaby Saddle
Multiples
(C)
Dipping and diverging reflection packages
Reduced imaging
CDP
Interval velocity (km s-1)
2.5 3.5 4.5 5.5 6.5 7.5
(D)
Fig. 8A
Fig. 8B
Fig. 8C
22°S
24°S
26°S
108°E
110°E
N
Elevation (km)
0 100 200 km

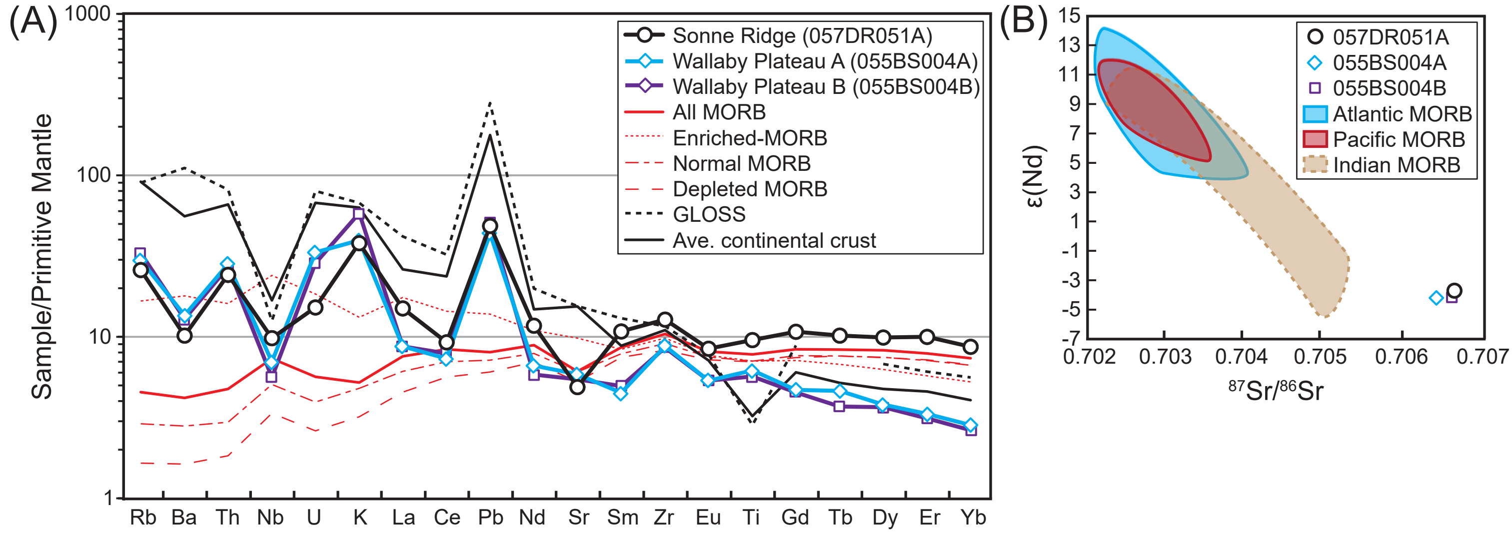
(A)
Sample/Primitive Mantle
1000
100
10
1
Sonne Ridge (057DR051A)
Wallaby Plateau A (055BS004A)
Wallaby Plateau B (055BS004B)
All MORB
Enriched-MORB
Normal MORB
Depleted MORB
GLOSS
Ave. continental crust
Rb
Ba
Th
Nb
U
K
La
Ce
Pb
Nd
Sr
Sm
Zr
Eu
Ti
Gd
Tb
Dy
Er
Yb
(B)
ε(Nd)
15
13
11
9
7
5
3
1
-1
-3
-5
-7
057DR051A
055BS004A
055BS004B
Atlantic MORB
Pacific MORB
Indian MORB
0.702
0.703
0.704
0.705
0.706
0.707
$^{87}Sr/^{86}Sr$

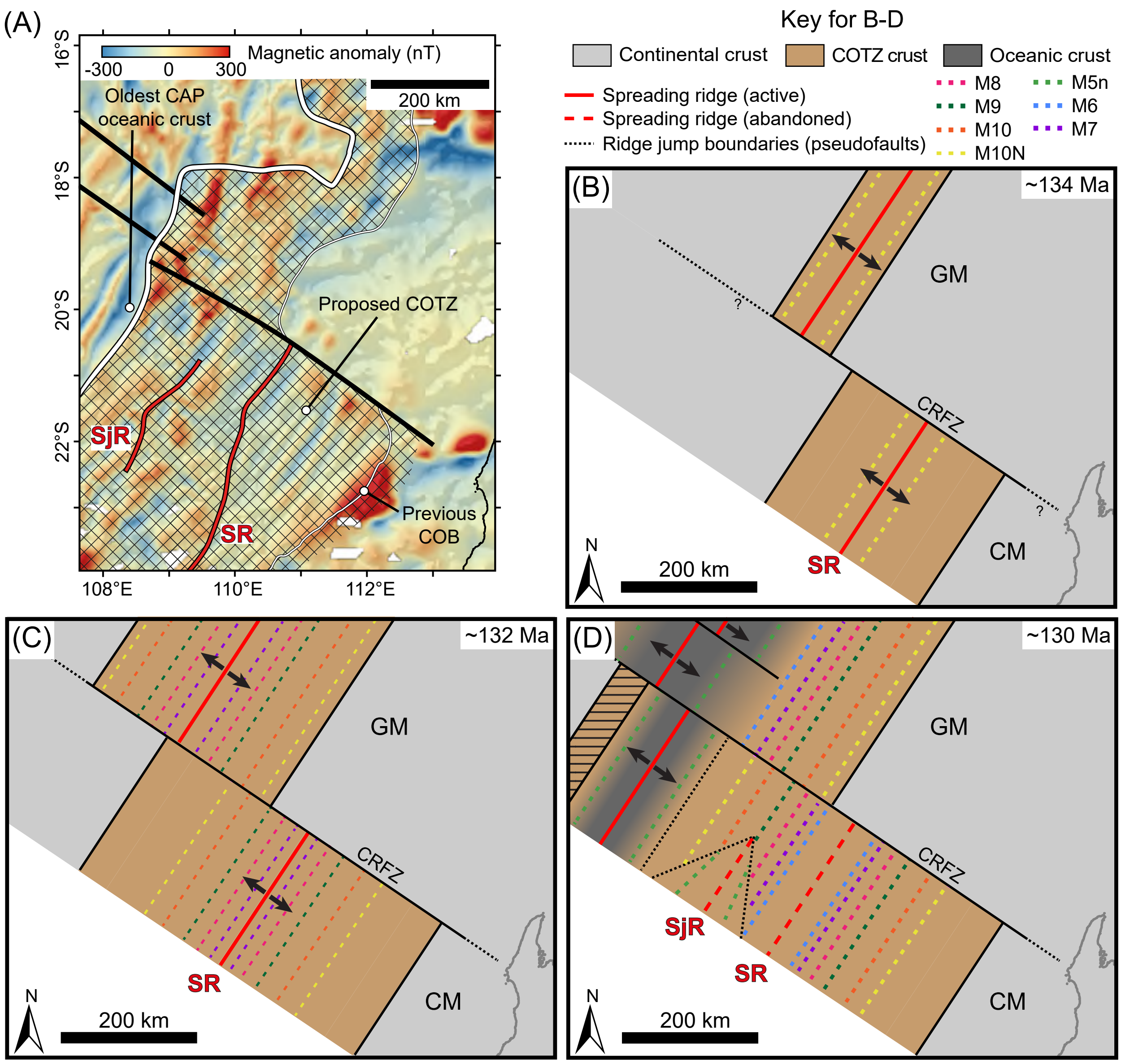
(A)
Magnetic anomaly (nT)
-300
0
300
200 km
Oldest CAP oceanic crust
Proposed COTZ
Previous COB
SjR
SR
16°S
18°S
20°S
22°S
108°E
110°E
112°E
Key for B-D
Continental crust
COTZ crust
Oceanic crust
Spreading ridge (active)
Spreading ridge (abandoned)
Ridge jump boundaries (pseudofaults)
M8
M9
M10
M10N
M5n
M6
M7
(B)
~134 Ma
GM
CRFZ
CM
SR
200 km
N
(C)
~132 Ma
GM
CRFZ
CM
SR
200 km
N
(D)
~130 Ma
GM
CRFZ
CM
SjR
SR
200 km
N